Assessment of CD37 B-cell antigen and cell-of-origin significantly improves risk prediction in diffuse large B-cell lymphoma

Zijun Y. Xu-Monette[1*], Ling Li[2*], John C. Byrd[3], Kausar J. Jabbar[1], Ganiraju C. Manyam[4], Charlotte Maria de Winde[5], Michiel van den Brand[5], Alexander Tzankov[6], Carlo Visco[7], Jing Wang[4], Karen Dybkaer[8], April Chiu[9], Attilio Orazi[10], Youli Zu[11], Govind Bhagat[12], Kristy L. Richards[13], Eric D. Hsi[14], William W.L. Choi[15], Jooryung Huh[16], Maurilio Ponzoni[17], Andrés J.M. Ferreri[17], Michael B. Møller[18], Ben M. Parsons[19], Jane N. Winter[20], Michael Wang[21], Frederick B. Hagemeister[21], Miguel A. Piris[22], J. Han van Krieken[5], L. Jeffrey Medeiros[1], Yong Li[23], Annemiek B. van Spriel[5] and Ken H. Young[1,24¶]

[1]Department of Hematopathology, The University of Texas MD Anderson Cancer Center, Houston, TX, USA; [2]Department of Oncology, The First Affiliated Hospital Zhengzhou University, Zhengzhou, China; [3] Department of Hematology and Oncology, The Ohio State University, Columbus, OH, USA; [4]Department of Bioinformatics and Computational Biology, The University of Texas MD Anderson Cancer Center, Houston, TX, USA; [5]Radboud Institute for Molecular Life Sciences, Radboud University Medical Center, Nijmegen, The Netherlands; [6]University Hospital, Basel, Switzerland; [7]San Bortolo Hospital, Vicenza, Italy; [8]Aalborg University Hospital, Aalborg, Denmark; [9]Memorial Sloan-Kettering Cancer Center, New York, NY, USA; [10]Weill Medical College of Cornell University, New York, NY, USA; [11]The Methodist Hospital, Houston, TX, USA; [12]Columbia University Medical Center and New York Presbyterian Hospital, New York, NY, USA; [13]University of North Carolina School of Medicine, Chapel Hill, NC, USA; [14]Cleveland Clinic, Cleveland, OH, USA; [15]University of Hong Kong Li Ka Shing Faculty of Medicine, Hong Kong, China; [16]Asan Medical Center, Ulsan University College of Medicine, Seoul, Korea; [17]San Raffaele H. Scientific Institute, Milan, Italy; [18]Odense University Hospital, Odense, Denmark; [19]Gundersen Lutheran Health System, La Crosse, WI, USA; [20]Feinberg School of Medicine, Northwestern University, Chicago, IL, USA; [21]Department of Lymphoma/Myeloma, The University of Texas MD Anderson Cancer Center, Houston, TX, USA; [22]Hospital Universitario Marqués de Valdecilla, Santander, Spain; [23]Department of Cancer Biology, Cleveland Clinic, Lerner Research Institute, Cleveland, OH; [24]The University of Texas School of Medicine, Graduate School of Biomedical Sciences, Houston, TX, USA

*These authors made equal contribution

Running head: CD37 is a critical determinant of R-CHOP outcome in DLBCL

Keywords: CD37, DLBCL, M-IPI-R, PD-1, ICOSLG, COO, IPI, R-CHOP, rituximab, CD20, CTLA-4, GCB, ABC

Abstract Word Count: 249

Main Text Word Count: 3,997

Number of Figures: 7

Number of Supplemental Figures: 6

Number of Tables: 5

Number of Supplemental Tables: 5

Number of References: 66

¶ Correspondence:

Ken H. Young, MD, PhD, The University of Texas MD Anderson Cancer Center, Department of Hematopathology, 1515 Holcombe Boulevard, Houston, Texas 77030-4009, USA. Phone: 1-713-745-2598; Fax: 1-713-792-7273; Email: khyoung@mdanderson.org;

Key Points:

- CD37 positivity predicts significantly better survival in DLBCL treated with R-CHOP, predominating other prognostic factors in GCB-DLBCL
- CD37 loss is a potent risk factor for R-CHOP resistance in both GCB- and ABC-DLBCL

Abstract

CD37 (tetraspanin TSPAN26) is a B-cell surface antigen widely expressed on mature B-cells. CD37 is involved in immune regulation and tumor suppression but its function has not been fully elucidated. In this study, we assessed CD37 expression in *de novo* diffuse large B-cell lymphoma (DLBCL), and investigated its clinical and biologic significance in 773 patients treated with rituximab-CHOP and 231 patients treated with CHOP chemotherapy. We found CD37 loss ($CD37^-$) in ~60% of DLBCL predicted significantly decreased survival rates in R-CHOP-treated patients, independent of the International Prognostic Index (IPI), germinal-center-B-cell–like (GCB)/activated-B-cell–like (ABC) cell-of-origin, nodal/extranodal primary origin, and the prognostic factors associated with $CD37^-$, including *TP53* mutation, NF-κB^{high}, Myc^{high}, p-$STAT3^{high}$, $survivin^{high}$, $p63^-$, and *BCL6* translocation. Conversely, CD37 positivity predicted superior survival, abolishing the prognostic impact of high IPI and above biomarkers in GCB-DLBCL but not in ABC-DLBCL. Combining $CD37^-$ status and ABC cell-of-origin risk scores with the IPI, defined as M-IPI-R (molecularly-adjusted-IPI-for-R-CHOP), or IPI-plus-immunohistochemistry for CD37, Myc, and Bcl-2 (defined as IPI+IHC), significantly improved risk prediction over IPI alone. Gene expression profiling suggested that decreased *CD20* and increased *PD-1* levels in $CD37^-$ DLBCL, *ICOSLG* upregulation in $CD37^+$ GCB-DLBCL, and CD37 functions during rituximab-CHOP treatment, underlie the pivotal role of CD37 signaling to clinical outcomes. In conclusion, CD37 is a critical determinant of rituximab-CHOP outcome in DLBCL especially in GCB-DLBCL, representing its importance for optimal rituximab action and

sustained immune responses. The combined molecular and clinical prognostic indices, M-IPI-R and IPI+IHC, have remarkable predictive values in rituximab-CHOP-treated DLBCL.

Introduction

The leukocyte surface antigen CD37 (TSPAN26), a member of the tetraspanin/tetraspan/transmembrane-4 superfamily, is widely expressed on normal and malignant mature B-cells and downregulated in plasma cells.[1-4] Most B-cell malignancies express CD37, including B-cell non-Hodgkin lymphoma (NHL) and B-cell chronic lymphocytic leukemia (CLL).[5] CD37 was detected at variable levels in 60% of Burkitt lymphoma cell lines.[6] Although CD37 expression in neoplastic B-cells correlated with the maturation stage of their corresponding B-cell counterparts, B-CLL has lower CD37 levels than do normal mature circulating B-lymphocytes.[3]

Tetraspanins are considered as "molecular facilitators" of signaling transduction, involved in a wide range of biological processes including cell growth, survival, adhesion, trafficking, intercellular communication via exosomes, metastasis, and immune responses.[1,4,7-9] CD37 forms complexes with other tetraspanins and major histocompatibility complex (MHC) class-II on B-cells. CD37 is important for T-cell–B-cell interaction, IgG/IgA production, and a balance between immune responses and tolerance,[1,2,4,10-13] although its role in adaptive immunity is controversal.[1,13-15] Using a *Cd37*$^{-/-}$ mouse model and a confirmative cohort of patients with diffuse large B-cell lymphoma (DLBCL), our study group recently showed that loss of CD37 and interaction between CD37 and SOCS3 leads to constitutive activation of the IL6-AKT-STAT3 pathway, spontaneous development of germinal center-derived lymphoma, and poorer clinical outcomes.[16]

CD37 could be targeted by monoclonal antibodies in patients with CLL and NHL expressing high levels of CD37. Although anti-CD37 antibody development predates rituximab (a chimeric monoclonal anti-CD20 IgG1 antibody) by nearly a decade, anti-CD37 antibodies (with otlertuzumab/TRU-016 most common) are in the spotlight only recently[1,5,17-20] and have

shown promise in phase I/II clinical trials for CLL and NHL.[1] Upon cross-ligation with anti-CD37 antibodies, CD37 transduces both death signals (from the N-terminal domain associated with SHP1, LYN, and PI3Kγ) and opposing survival signals (from the C-terminal domain recruiting p85 and PI3Kδ).[10]

DLBCL is the most common and heterogeneous NHL. Although the addition of rituximab (R-) to CHOP (cyclophosphamide, hydroxydaunorubicin/doxorubicin, Oncovin/vincristine, prednisone) significantly improves clinical outcomes, approximately one-third of DLBCL patients still have refractory disease or relapse.[21-23] Currently, DLBCL risk stratification relies mainly on the International Prognostic Index (IPI), which is based on patients' clinical features. However, the IPI cannot identify high-risk subgroups in the rituximab era,[24,25] since it was originally developed for CHOP outcome prediction from multivariate survival analyses in CHOP-treated patients.[26] Unfortunately, robust and reproducible biomarkers in DLBCL are also lacking.[27,28] Gene expression profiling (GEP) subdivides DLBCL into two major molecular subtypes, germinal-center-B-cell–like (GCB) DLBCL and activated-B-cell–like (ABC) DLBCL, and patients with ABC-DLBCL have poorer survival.[29] In ABC-DLBCL, B-cell receptor (BCR) signaling is chronically active with constitutive activation of antiapoptotic nuclear factor-kappaB (NF-κB); comparably, GCB-DLBCL has tonic BCR signaling with PI3K pathway activation (either proapoptotic or antiapoptotic).[30,31]

In this study, we assessed CD37 status and its prognostic effects in large cohorts of patients with DLBCL, and correlated CD37 status with tumor biology at both the protein and mRNA levels to determine the underlying mechanisms.

Methods

Patients

Totally 1,037 patients with *de novo* DLBCL were studied as a part of the International DLBCL R-CHOP Consortium Program, including 806 R-CHOP-treated patients (discovery cohort: n = 560, validation cohort: n = 246) and 231 CHOP-treated patients. The study was conducted in accordance with the Helsinki Declaration and was approved as being of minimal or no risk or as exempt by the institutional review boards of all participating medical centers.

Genetic and immunohistochemical analysis

Tissue microarrays prepared from the diagnostic formalin-fixed, paraffin-embedded (FFPE) blocks were stained with a CD37 monoclonal antibody (clone 2B8, Thermo Fisher Scientific).[16] FFPE tissue sections were also stained for IgA, IgG, IgM, p53, MDM2, p63, NF-κB subunits, p-STAT3, Myc, Bcl-2, Bcl-6, CD10, GCET1, FOXP1, MUM1/IRF4, BLIMP-1, Ki-67, CD5, CD30, CXCR4, PI3K, p-AKT, and survivin, and assessed for *TP53* mutations and *MYC*/*BCL2*/*BCL6* translocations, as described in the supplemental materials. GEP was performed on Affymetrix GeneChips HG-U133 Plus Version 2.0 (Affymetrix, Santa Clara, CA) using total RNAs extracted from FFPE tissues (GSE#31312).[32]

Statistical analysis

Correlations between CD37 and the clinical factors and biomarkers were analyzed using the chi-square test, Fisher's exact test, unpaired *t* test (2-tailed), and Spearman rank correlation. Survival analysis was performed using the Kaplan-Meier method and the log-rank (Cox-Mantel) test with GraphPad Prism 6 software. Overall survival (OS) was calculated from the date of diagnosis to the date of death from any cause or last follow-up for censored patients. Progression-free survival (PFS) was calculated from the date of diagnosis to the date of disease progression, recurrence, or death from any cause. Multivariate analysis was conducted using Cox proportional hazard regression models with SPSS software, version 19.0 (IBM, Armonk, NY). *P* values ≤0.05 were considered statistically significant.

Results

DLBCL patients with CD37 surface expression have significantly better clinical outcomes

CD37 surface expression was scored in 5% increments and CD37 staining was evaluable for 527 cases in the discovery cohort. Fig. 1A and B show representative CD37-negative ($CD37^-$) and CD37-positive ($CD37^+$) immunohistochemistry results, respectively. Staining for CD37 was positive (≥5%) at variable expression levels in 40% (212/527) of the discovery cohort (Fig. 1C). The ABC-DLBCL subgroup had a higher frequency of $CD37^+$ patients than the GCB-DLBCL subgroup (46.8% *vs*. 33.6%, Table 1), and a higher mean level of CD37 protein ($P = .002$; Figure 1D) and *CD37* mRNA ($P < .0001$; Supplemental Figure S1A). Cell-of-origin according to the B-cell-associated gene signatures classification[33] did not show significant differences between the $CD37^+$ and $CD37^-$ groups, although in the GCB subtype, $CD37^+$ DLBCL had a nonsignificantly higher frequency of centrocyte cell-of-origin (Supplemental Figure S1B).

At clinical presentation, patients with $CD37^-$ DLBCL had a higher frequency of ECOG performance status >1 than patients with $CD37^+$ DLBCL (20.6% *vs*. 10.7%, Table 1). Although the $CD37^+$ DLBCL group had a trend toward more elderly (≥60 years) patients ($P = .064$), these patients had a significantly higher complete response rate and significantly increased OS and PFS rates compared with the $CD37^-$ DLBCL patients ($P < .0001$; Figure 1E). The favorable effect of CD37 expression was independent of GCB/ABC subtype, high/low IPI, and nodal/extranodal primary origin (Figures 1F-H). Among the $CD37^+$ patients, CD37 high/low levels did not seem to be prognostic, although in some $CD37^+$ ABC-DLBCL patients with high CD37 levels, the favorable effect of CD37 expression was decreased (Supplemental Figure S1C). The significant impact of $CD37^{+/-}$ status was confirmed in an independent validation cohort (n = 246) ($P = .0003$ for OS and $P = .0065$ for PFS, Supplemental Figure S1D).

CD37 loss is associated with lower levels of *CD37* and *CD20* mRNA expression

CD37 mRNA levels were obtained from the GEP data and correlated with CD37 protein levels. The $CD37^+$ group had a significantly higher mean level of *CD37* mRNA than the $CD37^-$ group (Figure 2A). Employing the Spearman rank correlation method, CD37 protein and *CD37* mRNA levels were significantly correlated (r = 0.25, *P* = 7.57e-8). In addition, CD37 negativity was associated with downregulation of many BCR signaling–related genes (Table 2). *CD20*/*MS4A1* mRNA levels significantly correlated with both CD37 protein (r = 0.209, *P* = 8.16e-6) and *CD37* mRNA levels (r = 0.406, *P* = 3.40e-21), likely reflecting both CD37 and CD20 are expressed in mature B-cells with BCR and downregulated in plasma cells. Moreover, tested in 13 DLBCL cell lines, CD20 and CD37 protein levels measured by flow cytometry also showed significant correlation (Spearman rank correlation: r = 0.771, *P* = .002). In six cell lines ($CD20^-$/$CD37^-$: Oci-Ly19, SU-DHL6, WSU-NHL; $CD20^+$/$CD37^+$: Oci-Ly8, SU-DHL5, and SU-DHL2), CD20 and CD37 levels showed strong correlation, confirmed by two different CD37 monoclonal antibodies (WR17, HH1) (linear regression: R^2 = 0.9737, Figure 2B). As control, CD19 expression was also measured and detected on all DLBCL cell lines.

We further treated these six cell lines with rituximab (Rituxan and MabThera) and compared the cytotoxic effect. As expected, $CD20^-$/$CD37^-$/$CD19^+$ cell lines had less Rituxan-binding and were resistant to rituximab treatment in contrast to $CD20^+$/$CD37^+$/$CD19^+$ cell lines (Figure 2B, Supplemental Figure S2A). Likewise, in the discovery cohort, patients with lower (<mean) *CD20* mRNA levels had significantly poorer OS and PFS in the overall DLBCL and ABC-DLBCL cohorts, and poorer OS in the GCB-DLBCL cohort (Figure 2C).

In order to investigate whether CD37's prognostic significance was actually due to its association with *CD20* mRNA levels, firstly we incorporated both *CD20* mRNA and CD37 factors into the survival analysis (Figures 2D-E, Supplemental Figure S2B). We found $CD37^+$ status significantly predicted favorable OS and PFS regardless of high/low *CD20* mRNA levels;

furthermore, CD37^{+} DLBCL patients with low *CD20* mRNA levels still had significantly better OS and PFS than CD37^{-} DLBCL patients with high *CD20* mRNA levels, especially in cases of GCB-DLBCL. On the other hand, *CD20* mRNA levels only showed significant impact on OS and PFS in CD37^{-} DLBCL overall (but not in the GCB/ABC subset), and on PFS in the CD37^{+} ABC subgroup.

Secondly, to eliminate the confounding prognostic effects conferred by CD20, we studied CD37 expression in a CHOP-treated cohort (n = 231). We found CD37 positivity still correlated with significantly better survival, yet with less predictive power (P = .022 for OS and P = .013 for PFS), more significantly in GCB-DLBCL than in ABC-DLBCL (Supplemental Figure S3A). However, this favorable impact was limited in patients with relatively low CD37 levels (≤50%) while was lost in CD37^{high} (>50%) patients (Figure 3F). Comparing between CHOP-treated and R-CHOP-treated patients, CD37^{high} patients especially had improved survival with R-CHOP treatment regardless of *CD20* mRNA levels (Supplemental Figures S3B-C).

Together, these results suggest that although CD20 levels may partially contribute to the prognostic effects of CD37 status in CD37^{-} DLBCL and CD37^{+} ABC-DLBCL patients treated with R-CHOP, CD37 positivity predicts better survival (more remarkable in GCB-DLBCL), independent of CD20 expression, but to certain extent, dependent on the use of rituximab.

CD37 loss in DLBCL is associated with adverse prognostic factors, including *TP53* mutations, NF-κB activation, and *MYC* translocation

To get a better understanding of the underlying molecular mechanisms, we first correlated CD37 status with a spectrum of genetic/phenotypical biomarkers. Compared with the CD37^{+} group, the CD37^{-} group more frequently had GCB cell-of-origin, *TP53* mutation, *MYC* rearrangement, increased p50, RelB, and p65 (NF-κB) nuclear expression, and the IgA^{+}

immunophenotype. Conversely, the $CD37^+$ group more frequently had ABC cell-of-origin, $p63^+$, $PI3K^{high}$, $CXCR4^{high}$, $GCET1^{high}$, $FOXP1^{high}$, $MUM1/IRF4^{high}$, and the IgM^+ immunophenotype.

To eliminate the confounding effect of the GCB predominance in $CD37^-$ DLBCL on the molecular differences, we further compared the $CD37^-$ and $CD37^+$ groups in GCB-DLBCL and ABC-DLBCL separately. In GCB-DLBCL, $CD37^-$ was associated with *TP53* mutations and nuclear expression of p50, p65, Myc, and p-STAT3. In ABC-DLBCL, $CD37^-$ was associated with *BCL6* translocations and nuclear expression of p50, RelB, and survivin. In contrast, $CD37^+$ GCB-DLBCL was associated with GCET1 and BCL-6 expression, and $CD37^+$ ABC-DLBCL was associated with PI3K, CXCR4, GCET1, MUM1/IRF4 and FOXP1 expression (Figures 3A-B).

Predictive value of CD37 expression is robust, especially in GCB-DLBCL

To examine whether the adverse effect of CD37 loss depends on its associated molecular abnormalities and to identify prognostic determinants, we incorporate both CD37 and associated biomarkers into the survival analyses. As shown in Figure 3C and Supplemental Figure S4A, in GCB-DLBCL, CD37 loss correlated with significantly decreased PFS/OS rates with and without *TP53* mutation, $p50^{high}$, $p65^{high}$, Myc^{high}, $p\text{-}STAT3^{high}$, $GCET1^{low}$, $BCL\text{-}6^{low}$, and *MYC* rearrangement, although *TP53* mutation, *MYC* rearrangement, and Myc^{high} had additive adverse effects to CD37 loss. In particular, patients with $CD37^-$ GCB-DLBCL without *TP53* mutation, $p50^{high}$, and Myc^{high} expression (the 3 adverse factors most strongly associated with $CD37^-$ in GCB-DLBCL) remained to have significantly worse survival than patients with $CD37^+$ GCB-DLBCL (OS: $P = .0015$; PFS: $P = .0011$). Conversely, CD37 positivity robustly predicted significantly better survival in GCB-DLBCL. In fact, this predictive value completely abolished the prognostic significance of *TP53* mutation, $p50^{high}$, Myc^{high}, $p\text{-}STAT3^{high}$, and $GCET1^{high}$ expression in $CD37^+$ GCB-DLBCL, although not that of *MYC* rearrangement. Even more strikingly, the IPI lost prognostic significance in patients with $CD37^+$ GCB-DLBCL (Figure 3D).

Similarly, in ABC-DLBCL, CD37 loss predicted significantly worse survival with and without p50^{high}, survivin^{high}, RelB^{+}, p63^{-}, CXCR4^{high}, PI3K^{high}, FOXP1^{high}, MUM1^{high}, and *BCL6* translocations. In particular, patients with CD37^{-} ABC-DLBCL without p50^{high} and survivin^{high} expression (the two prognostic factors most strongly associated with CD37^{-} in ABC-DLBCL) still had significantly poorer survival than patients with CD37^{+} ABC-DLBCL (OS: $P = .0017$; PFS: $P = .0009$). However, ABC versus GCB subtype of CD37^{+} DLBCL patients had significantly worse survival (Figure 1F), and among CD37^{+} ABC-DLBCL patients, high IPI, *TP53* mutation, and Myc^{high} had significant adverse impact, in contrast to their lack of apparent effect in patients with CD37^{+} GCB-DLBCL (Figures 3E-F, Supplemental Figure S4B).

Multivariate survival analysis shows remarkable predictive values of CD37 status in GCB-DLBCL

We further performed multivariate survival analysis for CD37$^{-/+}$ status using Cox regression models. After adjustment of clinical variables and CD37 status-associated prognostic factors, CD37 status remained to be a significant prognostic factor in overall DLBCL, GCB-DLBCL and ABC-DLBCL. CD37^{-} status had the most significant risk prediction power among all the molecular biomarkers in the Cox model for DLBCL overall (for OS, hazard ratio [HR]: 3.43; 95% confidence interval [CI]; 1.96-6.02; $P < .001$; for PFS, HR: 3.91; 95% CI: 2.28-6.71; $P < .001$), followed by ABC cell-of-origin (Table 3).

Impressively, in patients with GCB-DLBCL, the HR of CD37^{-} was even higher than that of IPI >2 (for OS, 4.86 *vs.* 3.66; for PFS, 5.64 *vs.* 3.39), and the IPI lost prognostic significance in CD37^{+} GCB-DLBCL (Table 3). Moreover, in both CD37^{+} and CD37^{-} GCB-DLBCL subsets, all biomarkers except Myc^{high} lost significance as independent factors for poorer survival. Differently, in CD37^{+} ABC-DLBCL, IPI >2, *TP53* mutations, Myc^{high}, p63^{-}, and survivin^{high} had

significant independent adverse impact, and in CD37^{-} ABC-DLBCL, IPI >2, p50^{high}, p63^{-}, and CXCR4^{high} were significant independent adverse prognostic factors (Supplemental Table S1).

Molecularly-adjusted-IPI-for-R-CHOP significantly improves risk stratification in DLBCL

Because CD37 status and GCB/ABC cell-of-origin showed remarkable prognostic significance independent of the IPI, we tested whether combining these two risk factors with the IPI improved the prognostic prediction. The IPI did separate the discovery cohort into four groups but had limited power to identify high-risk patients (15.2% of the discovery cohort; P = 0.073 [OS] and 0.017 [PFS] compared with intermediate-high-risk patients) (Figure 4A). We added the scores for CD37 status (add 1 point if CD37^{-}) and cell-of-origin (add 1 point if ABC) to the IPI, resulting in a "molecularly adjusted IPI for R-CHOP" (M-IPI-R) score for each patient. This "M-IPI-R" could redistribute patients into four groups (low-risk: score 0-1 [16.6%]; intermediate-risk: score 2-3 [42.7%]; high-risk: score 4-5 [34.6%]; and very-high-risk: score 6-7 [6.2%]), and showed significantly improved stratification power compared with the traditional IPI and cell-of-origin-adjusted-IPI (Supplemental Figure S5A) scores in separating high-risk and very-high-risk patients from intermediate-risk patients ($P < .0001$) (Figure 4B). The five-year OS rates for high-risk and very-high-risk groups were 40.19% and 18.06%, respectively, compared to 38.38% for the high-risk group identified by the traditional IPI.

Within the M-IPI-R-defined risk groups, GCB/ABC was not prognostic anymore but CD37^{-} status still showed significant adverse impact (Supplemental Figure S5B). Therefore we assigned 1 additional point for CD37^{-} into the "M-IPI-R", and found neither CD37$^{+/-}$ nor GCB/ABC had further prognostic significance within the newly defined risk groups. This version of "M-IPI-R", which may have fully adjusted the risk conferred by CD37^{-}, could refine the stratification into 5 different risk groups (Figure 4B): low-risk: score 0-1 (11.5%); low-intermediate-risk: score 2-3 (33.3%); intermediate-risk: score 4 (20.6%); high-risk: score 5-6

(28.7%); and very-high-risk group: score 7-8 (5.9%). The five-year OS rates for the high-risk and very-high-risk groups were 37.33% and 19.64%, respectively.

To develop a more applicable immunohistochemistry-based index, we tested various biomarkers and found combining $CD37^{-}$, Myc^{high}, and $Bcl\text{-}2^{high}$ risk factors with the IPI, defined as "IPI-plus-immunohistochemistry" (IPI+IHC), showed the strongest stratification power without redundancy (Supplemental Figure S5C: 1 point for $CD37^{-}$, and Figure 4C: 3 points for $CD37^{-}$). In Figure 4C, the five-year OS rates for high-risk (score 7-8, 16.3%) and very-high-risk (score 9-10, 3.5%) groups were 24.21% and 7.81%, respectively.

GEP analysis suggests roles of CD37 in immune signaling

We compared gene expression profiles of $CD37^{+}$ and $CD37^{-}$ groups in the discovery DLBCL cohort. Surprisingly, no significant CD37 gene signatures were identified in GCB-DLBCL although CD37 status had remarkable prognostic significance. In overall- and ABC-DLBCL only weak CD37 signatures were identified (Table 4, Supplemental Table S2), but these signatures were also heterogeneously expressed within both the $CD37^{+}$ and $CD37^{-}$ subgroups (Figure 5A).

Further gene set enrichment analysis showed that 48 and 125 gene sets were enriched in $CD37^{-}$ DLBCL and in $CD37^{-}$ ABC-DLBCL (false discovery rate [FDR] <0.25, Supplemental Tables S3-4), respectively, whereas no KEGG pathways were enriched in $CD37^{+}$ DLBCL or $CD37^{+}$ ABC-DLBCL significantly. Most gene sets enriched in $CD37^{-}$ DLBCL and $CD37^{-}$ ABC-DLBCL were related to infection (e.g., pertussis, salmonella, *Helicobacter pylori*, and prion disease) and immune signaling, including NOD-like receptor signaling, phagosome, chemokine signaling (Figures 5B-C), osteoclast differentiation, TOLL-like receptor signaling, and TNF signaling pathway among the top enriched gene sets.

Interestingly, a more distinct CD37 gene signature was identified in the PI3K^{high} but not PI3K^{low} ABC-DLBCL subset (Figure 5D), suggesting PI3K-involved CD37 signaling in ABC-DLBCL.[10] With FDR <0.05, 26 genes were upregulated in CD37^{+}/PI3K^{high} compared with CD37^{-}/PI3K^{high} ABC-DLBCL, including *BCL11A*, *PAX5*, *TCF4*, and *CLECL1* which functions as a T-cell costimulatory molecule. Paradoxically, tumor suppressors *EPB41L3* and *BCL11B*, *DRAM1* which is critical for p53-mediated apoptosis,[34] and *SAMSN1* (a negative regulator of B-cell activation and proliferation) were downregulated in CD37^{+}/PI3K^{high} ABC-DLBCL. Conversely, 225 genes were upregulated in CD37^{-}/PI3K^{high} compared with CD37^{+}/PI3K^{high} ABC-DLBCL, including many related to immune signaling. Of note, *CD163* (3.27-fold) is a marker of M2 (tumor-promoting) macrophage,[35] *CD14* (1.53-fold) is a marker for macrophage activation, *SERPING1* inhibits C1 complex in complement activation, *LILRB2* (1.83-fold) encodes a leukocyte immunoglobulin-like receptor that negatively regulates MHC-I-mediated antigen presentation and immune responses leading to tolerance development,[36,37] and *CD300A* (1.98-fold) inhibits the antitumor activities by natural killer and mast cells[38,39] (Table 4, Supplemental Table S5).

Different from CD37$^{+/-}$ status only showing a weak GEP signature, GCB/ABC cell-of-origin showed remarkable GEP signatures in both the CD37^{+} DLBCL and CD37^{-} DLBCL subsets (Figures 5E-F): 2346 significant transcripts in CD37^{+} DLBCL and 1383 transcripts in CD37^{-} DLBCL with FDR <0.01 (Table 4: >2 fold difference). In both CD37^{-} and CD37^{+} DLBCL subsets, ABC compared with GCB cell-of-origin had significant upregulation of *TNFRSF13B*/*TACI* (receptor for TNFSF13/APRIL and TNFSF13B/BAFF), *IGHM*, *CLECL1*, *MIR155HG*, *IRF4*, *BATF*, and *CCL8*. Additionally, in the CD37^{+} subset, ABC- compared with GCB-DLBCL had significant upregulation of *FOXP1* and *AICDA*, whereas downregulation of *HLA-DOB*, *LRMP* (which plays a role in the delivery of peptides to MHC-I), and *LMO2*. In the CD37^{-} subset, ABC compared with GCB cell-of-origin had significant *LILRB2* upregulation.

CD37 may play important roles in the costimulatory and PD-1 pathways

We compared the expression of important immune genes between $CD37^-$ and $CD37^+$ patients and within the $CD37^-$ and $CD37^+$ subsets (Table 5). In GCB-DLBCL, $CD37^+$ status, which robustly predicted favorable clinical outcomes, correlated with *ICOSLG* (encoding ICOSL/ICOSLG,[40] the ligand for the T-cell-specific receptor ICOS) upregulation, whereas CD37 loss in ABC-DLBCL correlated with *PDCD1*/*PD-1* upregulation (engagement of PD-1 on T-cells with its ligand PD-L1 on tumor cells inhibits T-cell antitumor responses) (Figures 6A-B). In $p50^{high}$ DLBCL, $CD37^-$ correlated with *PD-1* upregulation in both GCB- and ABC-DLBCL (Figure 6C). Immunohistochemical analysis for PD-1 expression (unpublished preliminary data) further confirmed the significant association of CD37 loss with PD-1 overexpression in DLBCL (Figures 6D-E), with significant or borderline *P* values in the ABC and GCB subsets.

ABC versus GCB cell-of-origin correlated with *ICOSLG* downregulation ($P < .0001$) and *IL10RA*/*IL10*[41] and *LILRB*/*A* upregulation in both $CD37^-$ and $CD37^+$ subsets, and with *CD274* and *PDCD1LG2* (encoding the PD-1 ligands PD-L1 and PD-L2,[42] respectively) upregulation in the $CD37^-$ subset (also in overall DLBCL) (Figure 6F). Immune dysregulation was also found in subsets with *TP53* mutations, Myc^{high}, $p50^{high}$, $p\text{-}STAT3^{high}$, $FOXP1^{high}$, $MUM1/IRF4^{high}$, or $CXCR4^{high}$ (e.g., upregulation of *PD-L1*/*L2*, *CTLA4*, *TIM3*, *LILRB2*, *IL6R*, and *IL10RB*, whereas downregulation of *ICOSLG*, *CD58*, and *MHC-I*/*II*) (Figure 7, Supplemental Figure S6).

Discussion

In this study we demonstrated the robust prognostic value of CD37 status in a large cohort of DLBCL. Integrating assessment of CD37 status and GCB/ABC cell-of-origin into the IPI calculation (M-IPI-R) markedly improved the predicative power of IPI in R-CHOP-treated DLBCL patients. However, currently GCB/ABC classification is not yet the standard of care,

although it may be in the future.[43] Respecting this, immunohistochemistry for Myc and Bcl-2 may be an alternative for GCB/ABC determination in the M-IPI-R.

The pivotal role of $CD37^{+/-}$ status for prognosis has two aspects. First, CD37 positivity is an independent predictor of favorable outcome in R-CHOP-treated DLBCL patients. CD37 ligation experiments have shown that CD37 can function as a death receptor in B-cells.[10] Upon cross-ligation, CD37 translocates into the membrane lipid rafts, becomes associated with SHP1, LYN, and SYK recruiting PI3Kγ, and transduces signaling favoring cellular death.[10] Considering the somehow R-CHOP-specific but *CD20*-independent prognostic significance of CD37 expression (Figure 2), and the lack of a prominent $CD37^{+}$ GEP signature at diagnosis, we speculated that CD37 might act as a "molecular facilitator" of rituximab action during R-CHOP treatment, especially for antibody-dependent cellular cytotoxicity, cross-linking, aggregation in lipid rafts thereby transactivating tyrosine kinases, apoptosis induction, and long-term T-cell responses (Figure 7, I).[44-46] Remarkably, such potential CD37-rituximab signaling could abolish the adverse impact of many prognostic factors and even that of high IPI scores in GCB-DLBCL, but not in ABC-DLBCL however, even though there was no significant difference in *CD20* mRNA levels between GCB-DLBCL and ABC-DLBCL (Supplemental Figure S2B). The enhanced antitumor effect by $CD37^{+}$ might have been dampened in ABC-DLBCL by *ICOSLG* downregulation, and upregulation of *TNFRSF13B/TACI*, *PD-L1*, *AICDA*, *IL10*/*IL10RA*, and *LILRA*/*B*, increased FOXP1 and IRF4 levels which suppress MHC-II expression, chronic active BCR signaling, and apoptosis-suppressive mechanisms (e.g., *DRAM1*, *EPB41L3*, and *BCL11B* were downregulated in $CD37^{+}$/$PI3K^{high}$ ABC-DLBCL).[47,48] Of note, *TNFRSF13B*/*TACI* suppresses *ICOSLG* and *BIM* (proapoptotic) expression.[49]

Secondly, CD37 loss independently predicted significantly worse survival in DLBCL. Increased PD-1 whereas decreased *ICOSLG* and *CD20* expression,[50-56] may contribute to the poor clinical outcome of $CD37^{-}$ patients (Figure 7, II). *CD20* downregulation could be due to

cell-of-origin[57,58] of CD37$^-$ DLBCL cells or increased cytokines which was reported to suppress CD20 expression.[59] In addition, many *FCGR* genes were upregulated in CD37$^-$ DLBCL especially in p50^{high}/CD37$^-$ DLBCL, suggesting the potential for trogocytosis (the transfer of rituximab-CD20 complexes from tumor cells to Fc receptor–bearing cells[53]) and R-CHOP resistance. Previous studies have demonstrated that CD37 has a role in T-cell–B-cell interaction and humoral responses, which can be observed under suboptimal costimulatory conditions,[11] and that *Cd37*$^{-/-}$ mice develop germinal center–derived lymphomas.[16] In this study, CD37$^-$ DLBCL was enriched with gene sets related to infection and immune signaling and presence of oncogenic drivers, which might result from loss of CD37's antitumor function during lymphomagenesis (potentially also after R-CHOP treatment).

These results also have therapeutic implications. For CD37$^+$ ABC-DLBCL with higher CD37 (but not CD20) expression, anti-CD37 antibody alone or combined with rituximab may have higher efficacy. Clinical outcomes may be further improved by combining with BTK inhibitors that inhibit BCR and CXCR4 signaling,[60] PD-L1 inhibitors, ICOS agonists, and immunoregulatory lenalidomide.[28,40,61] For CD37$^-$ DLBCL with immunosuppressive mechanisms and decreased CD20 levels, PD-1 blockade and ICOS agonists may be effective, as well as other targeted agents in p50^{high}, Myc^{high}, p-STAT3^{high}, or ABC subgroups of CD37$^-$ DLBCL (Figure 7).[62,63] Notably, Hodgkin and Reed-Sternberg cells which are thought to originate from pro-apoptotic germinal center B-cells but are rescued by acquired survival mechanisms, also show loss of CD20, CD37, and BCR and demonstrate particular sensitivity to immune-checkpoint blockade.[64-66]

In summary, in this study we established CD37$^{-/+}$ status as a robust biomarker and introduced two novel prognostic indices, M-IPI-R and IPI+IHC, for risk prediction in R-CHOP-treated DLBCL. Whether these indices can be useful prognostic tools in the clinic needs to be validated by future prospective studies. GEP analysis indicates novel strategies are needed

especially immunotherapies for $CD37^-$ DLBCL and anti-CD37 antibodies for $CD37^+$ ABC-DLBCL. Our findings from human samples are also valuable for understanding DLBCL pathogenesis and heterogeneity and have important clinical implications.

Acknowledgments

This study is supported by National Cancer Institute and National Institutes of Health grants (R01CA138688 and R01CA187415 to YL and KHY). ABvS is supported by the Netherlands Organization for Scientific Research (NWO-ALW VIDI Grant 864.11.006) and the Dutch Cancer Society (KUN2014-6845). KHY is also supported by The University of Texas MD Anderson Cancer Center Lymphoma Moonshot Program, Institutional Research Grant Award, an MD Anderson Lymphoma Specialized Programs of Research Excellence (SPORE) Research Development Program Award, and an MD Anderson Myeloma SPORE Research Developmental Program Award. KHY receives research support from Roche Molecular System, Gilead Sciences Pharmaceutical, Seattle Genetics, Dai Sanyo Pharmaceutical, Adaptive Biotechnology, Incyte Pharmaceutical, and HTG Molecular Diagnostics. The study is also partially supported by P50CA136411 and P50CA142509 and the MD Anderson Cancer Center Support Grant CA016672.

Authorship

Conception and design: ZYXM, KHY. **Research performance**: ZYXM, KJJ, CMW, MB, ABvS, KHY. **Provision of study thought, materials, key reagents and technology**: ZYXM, LL, JCB, LD, AT, XW, GCM, CV, JW, SMM, KD, AC, AO, YZ, GB, KLR, EDH, WWLC, JH, MP, AJMF, BMP, MBM, JNW, MW, FH, MAP,JHK, LJM, YL, ABS, KHY. **Collection and assembly of data under approved IRB and Material Transfer Agreement**: ZYXM, AT, CV, KD, AC, AO, YZ,

GB, KLR, EDH, WWLC, JHK, JH, MP, AJMF, BMP, MBM, JNW, MAP, KHY. **Data analysis and interpretation**: ZYXM, LL, JCB, YL, ABvS, KHY. **Manuscript writing**: ZYXM, KHY. **Final approval of manuscript:** All authors.

Conflicts of interest disclosure

The authors declare no conflicts of interest.

References

1. Beckwith KA, Byrd JC, Muthusamy N. Tetraspanins as therapeutic targets in hematological malignancy: a concise review. *Front Physiol*. 2015;6:91.
2. van Spriel AB. Tetraspanins in the humoral immune response. *Biochem Soc Trans*. 2011;39(2):512-517.
3. Barrena S, Almeida J, Yunta M, et al. Aberrant expression of tetraspanin molecules in B-cell chronic lymphoproliferative disorders and its correlation with normal B-cell maturation. *Leukemia*. 2005;19(8):1376-1383.
4. van Spriel AB, de Keijzer S, van der Schaaf A, et al. The tetraspanin CD37 orchestrates the alpha(4)beta(1) integrin-Akt signaling axis and supports long-lived plasma cell survival. *Sci Signal*. 2012;5(250):ra82.
5. Deckert J, Park PU, Chicklas S, et al. A novel anti-CD37 antibody-drug conjugate with multiple anti-tumor mechanisms for the treatment of B-cell malignancies. *Blood*. 2013;122(20):3500-3510.
6. Ferrer M, Yunta M, Lazo PA. Pattern of expression of tetraspanin antigen genes in Burkitt lymphoma cell lines. *Clin Exp Immunol*. 1998;113(3):346-352.
7. Zoller M. Tetraspanins: push and pull in suppressing and promoting metastasis. *Nat Rev Cancer*. 2009;9(1):40-55.
8. Andreu Z, Yanez-Mo M. Tetraspanins in extracellular vesicle formation and function. *Front Immunol*. 2014;5:442.
9. Escola JM, Kleijmeer MJ, Stoorvogel W, et al. Selective enrichment of tetraspan proteins on the internal vesicles of multivesicular endosomes and on exosomes secreted by human B-lymphocytes. *J Biol Chem*. 1998;273(32):20121-20127.
10. Lapalombella R, Yeh YY, Wang L, et al. Tetraspanin CD37 directly mediates transduction of survival and apoptotic signals. *Cancer Cell*. 2012;21(5):694-708.
11. Knobeloch KP, Wright MD, Ochsenbein AF, et al. Targeted inactivation of the tetraspanin CD37 impairs T-cell-dependent B-cell response under suboptimal costimulatory conditions. *Mol Cell Biol*. 2000;20(15):5363-5369.
12. van Spriel AB, Sofi M, Gartlan KH, et al. The tetraspanin protein CD37 regulates IgA responses and anti-fungal immunity. *PLoS Pathog*. 2009;5(3):e1000338.
13. van Spriel AB, Puls KL, Sofi M, et al. A regulatory role for CD37 in T cell proliferation. *J Immunol*. 2004;172(5):2953-2961.
14. Gartlan KH, Wee JL, Demaria MC, et al. Tetraspanin CD37 contributes to the initiation of cellular immunity by promoting dendritic cell migration. *Eur J Immunol*. 2013;43(5):1208-1219.
15. Sheng KC, van Spriel AB, Gartlan KH, et al. Tetraspanins CD37 and CD151 differentially regulate Ag presentation and T-cell co-stimulation by DC. *Eur J Immunol*. 2009;39(1):50-55.
16. de Winde CM, Veenbergen S, Young KH, et al. Tetraspanin CD37 protects against the development of B cell lymphoma. *J Clin Invest*. 2016;126(2):653-666.
17. Byrd JC, Pagel JM, Awan FT, et al. A phase 1 study evaluating the safety and tolerability of otlertuzumab, an anti-CD37 mono-specific ADAPTIR therapeutic protein in chronic lymphocytic leukemia. *Blood*. 2014;123(9):1302-1308.
18. Zhao X, Lapalombella R, Joshi T, et al. Targeting CD37-positive lymphoid malignancies with a novel engineered small modular immunopharmaceutical. *Blood*. 2007;110(7):2569-2577.
19. Heider KH, Kiefer K, Zenz T, et al. A novel Fc-engineered monoclonal antibody to CD37 with enhanced ADCC and high proapoptotic activity for treatment of B-cell malignancies. *Blood*. 2011;118(15):4159-4168.

20. Pagel JM, Spurgeon SE, Byrd JC, et al. Otlertuzumab (TRU-016), an anti-CD37 monospecific ADAPTIR() therapeutic protein, for relapsed or refractory NHL patients. *Br J Haematol*. 2015;168(1):38-45.

21. Friedberg JW. Relapsed/refractory diffuse large B-cell lymphoma. *Hematology Am Soc Hematol Educ Program*. 2011;2011:498-505.

22. Plosker GL, Figgitt DP. Rituximab: a review of its use in non-Hodgkin's lymphoma and chronic lymphocytic leukaemia. *Drugs*. 2003;63(8):803-843.

23. Ziepert M, Hasenclever D, Kuhnt E, et al. Standard International prognostic index remains a valid predictor of outcome for patients with aggressive CD20+ B-cell lymphoma in the rituximab era. *J Clin Oncol*. 2010;28(14):2373-2380.

24. Sehn LH, Berry B, Chhanabhai M, et al. The revised International Prognostic Index (R-IPI) is a better predictor of outcome than the standard IPI for patients with diffuse large B-cell lymphoma treated with R-CHOP. *Blood*. 2007;109(5):1857-1861.

25. Zhou Z, Sehn LH, Rademaker AW, et al. An enhanced International Prognostic Index (NCCN-IPI) for patients with diffuse large B-cell lymphoma treated in the rituximab era. *Blood*. 2014;123(6):837-842.

26. A predictive model for aggressive non-Hodgkin's lymphoma. The International Non-Hodgkin's Lymphoma Prognostic Factors Project. *N.Engl.J.Med.* 1993;329(14):987-994.

27. Sehn LH. Paramount prognostic factors that guide therapeutic strategies in diffuse large B-cell lymphoma. *Hematology Am Soc Hematol Educ Program*. 2012;2012(402-409.

28. Vaidya R, Witzig TE. Prognostic factors for diffuse large B-cell lymphoma in the R(X)CHOP era. *Ann Oncol*. 2014;25(11):2124-2133.

29. Alizadeh AA, Eisen MB, Davis RE, et al. Distinct types of diffuse large B-cell lymphoma identified by gene expression profiling. *Nature*. 2000;403(6769):503-511.

30. Young RM, Shaffer AL, 3rd, Phelan JD, Staudt LM. B-cell receptor signaling in diffuse large B-cell lymphoma. *Semin Hematol*. 2015;52(2):77-85.

31. Chen L, Monti S, Juszczynski P, et al. SYK inhibition modulates distinct PI3K/AKT- dependent survival pathways and cholesterol biosynthesis in diffuse large B cell lymphomas. *Cancer Cell*. 2013;23(6):826-838.

32. Visco C, Li Y, Xu-Monette ZY, et al. Comprehensive gene expression profiling and immunohistochemical studies support application of immunophenotypic algorithm for molecular subtype classification in diffuse large B-cell lymphoma: a report from the International DLBCL Rituximab-CHOP Consortium Program Study. *Leukemia*. 2012;26(9):2103-2113.

33. Dybkaer K, Bogsted M, Falgreen S, et al. Diffuse large B-cell lymphoma classification system that associates normal B-cell subset phenotypes with prognosis. *J Clin Oncol*. 2015;33(12):1379-1388.

34. Crighton D, Wilkinson S, O'Prey J, et al. DRAM, a p53-induced modulator of autophagy, is critical for apoptosis. *Cell*. 2006;126(1):121-134.

35. Nam SJ, Go H, Paik JH, et al. An increase of M2 macrophages predicts poor prognosis in patients with diffuse large B-cell lymphoma treated with rituximab, cyclophosphamide, doxorubicin, vincristine and prednisone. *Leuk Lymphoma*. 2014;55(11):2466-76.

36. Brown DP, Jones DC, Anderson KJ, et al. The inhibitory receptor LILRB4 (ILT3) modulates antigen presenting cell phenotype and, along with LILRB2 (ILT4), is upregulated in response to Salmonella infection. *BMC Immunol*. 2009;10:56.

37. Zhang P, Yu S, Li H, et al. ILT4 drives B7-H3 expression via PI3K/AKT/mTOR signalling and ILT4/B7-H3 co-expression correlates with poor prognosis in non-small cell lung cancer. *FEBS Lett*. 2015;589(17):2248-2256.

38. Lankry D, Rovis TL, Jonjic S, Mandelboim O. The interaction between CD300a and phosphatidylserine inhibits tumor cell killing by NK cells. *Eur J Immunol*. 2013;43(8):2151-2161.

39. Nakahashi-Oda C, Tahara-Hanaoka S, Shoji M, et al. Apoptotic cells suppress mast cell inflammatory responses via the CD300a immunoreceptor. *J Exp Med*. 2012;209(8):1493-1503.

40. Fan X, Quezada SA, Sepulveda MA, Sharma P, Allison JP. Engagement of the ICOS pathway markedly enhances efficacy of CTLA-4 blockade in cancer immunotherapy. *J Exp Med*. 2014;211(4):715-725.

41. Wolfle SJ, Strebovsky J, Bartz H, et al. PD-L1 expression on tolerogenic APCs is controlled by STAT-3. *Eur J Immunol*. 2011;41(2):413-424.

42. Rozali EN, Hato SV, Robinson BW, Lake RA, Lesterhuis WJ. Programmed death ligand 2 in cancer-induced immune suppression. *Clin Dev Immunol*. 2012;2012:656340.

43. Scott DW, Mottok A, Ennishi D, et al. Prognostic Significance of Diffuse Large B-Cell Lymphoma Cell of Origin Determined by Digital Gene Expression in Formalin-Fixed Paraffin-Embedded Tissue Biopsies. *J Clin Oncol*. 2015;33(26):2848-2856.

44. Smith MR. Rituximab (monoclonal anti-CD20 antibody): mechanisms of action and resistance. *Oncogene*. 2003;22(47):7359-7368.

45. Deans JP, Li H, Polyak MJ. CD20-mediated apoptosis: signalling through lipid rafts. *Immunology*. 2002;107(2):176-182.

46. Boross P, Leusen JH. Mechanisms of action of CD20 antibodies. *Am J Cancer Res*. 2012;2(6):676-690.

47. Brown PJ, Wong KK, Felce SL, et al. FOXP1 suppresses immune response signatures and MHC class II expression in activated B-cell-like diffuse large B-cell lymphomas. *Leukemia*. 2016;30(3):605-616.

48. Pan H, O'Brien TF, Wright G, et al. Critical role of the tumor suppressor tuberous sclerosis complex 1 in dendritic cell activation of CD4 T cells by promoting MHC class II expression via IRF4 and CIITA. *J Immunol*. 2013;191(2):699-707.

49. Zhang Y, Li J, Zhang YM, Zhang XM, Tao J. Effect of TACI signaling on humoral immunity and autoimmune diseases. *J Immunol Res*. 2015;2015:247426.

50. Kuijpers TW, Bende RJ, Baars PA, et al. CD20 deficiency in humans results in impaired T cell-independent antibody responses. *J Clin Invest*. 2010;120(1):214-222.

51. Kennedy GA, Tey SK, Cobcroft R, et al. Incidence and nature of CD20-negative relapses following rituximab therapy in aggressive B-cell non-Hodgkin's lymphoma: a retrospective review. *Br J Haematol*. 2002;119(2):412-416.

52. Bojarczuk K, Siernicka M, Dwojak M, et al. B-cell receptor pathway inhibitors affect CD20 levels and impair antitumor activity of anti-CD20 monoclonal antibodies. *Leukemia*. 2014;28(5):1163-1167.

53. Skarzynski M, Niemann CU, Lee YS, et al. Interactions between Ibrutinib and Anti-CD20 Antibodies: Competing Effects on the Outcome of Combination Therapy. *Clin Cancer Res*. 2016;22(1):86-95.

54. Johnson NA, Boyle M, Bashashati A, et al. Diffuse large B-cell lymphoma: reduced CD20 expression is associated with an inferior survival. *Blood*. 2009;113(16):3773-3780.

55. Suzuki Y, Yoshida T, Wang G, et al. Association of CD20 levels with clinicopathological parameters and its prognostic significance for patients with DLBCL. *Ann Hematol*. 2012;91(7):997-1005.

56. Tokunaga T, Tomita A, Sugimoto K, et al. De novo diffuse large B-cell lymphoma with a CD20 immunohistochemistry-positive and flow cytometry-negative phenotype: molecular mechanisms and correlation with rituximab sensitivity. *Cancer Sci*. 2014;105(1):35-43.

57. Batista FD, Harwood NE. The who, how and where of antigen presentation to B cells. *Nat Rev Immunol*. 2009;9(1):15-27.

58. Goenka R, Scholz JL, Sindhava VJ, Cancro MP. New roles for the BLyS/BAFF family in antigen-experienced B cell niches. *Cytokine Growth Factor Rev*. 2014;25(2):107-113.

59. Frank RR, Jagan S, Paganessi LA, et al. CD20, CD22, CD23, but Not CD37 Expression on CD19+ B-Cells Is Altered by Exogenous Factors in a Sub-Population of Chronic Lymphocytic Leukemia/Small Lymphocytic Leukemia (CLL/SLL) Patients. *Blood*. 2011;118(21):Abstract [3685].

60. Chen SS, Chang BY, Chang S, et al. BTK inhibition results in impaired CXCR4 chemokine receptor surface expression, signaling and function in chronic lymphocytic leukemia. *Leukemia*. 2016;30(4):833-843.

61. Nowakowski GS, LaPlant B, Macon WR, et al. Lenalidomide combined with R-CHOP overcomes negative prognostic impact of non-germinal center B-cell phenotype in newly diagnosed diffuse large B-Cell lymphoma: a phase II study. *J Clin Oncol*. 2015;33(3):251-257.

62. Drake CG, Lipson EJ, Brahmer JR. Breathing new life into immunotherapy: review of melanoma, lung and kidney cancer. *Nat Rev Clin Oncol*. 2014;11(1):24-37.

63. Gajewski TF, Schreiber H, Fu YX. Innate and adaptive immune cells in the tumor microenvironment. *Nat Immunol*. 2013;14(10):1014-1022.

64. Rosenwald A, Kuppers R. Pathology and molecular pathology of Hodgkin lymphoma, in Engert A, Younes A (ed): Hodgkin Lymphoma: A Comprehensive Overview (ed 2). Springer International Publishing, 2015, pp 45-64.

65. Armand P. Immune checkpoint blockade in hematologic malignancies. *Blood*. 2015;125(22):3393-3400.

66. Thanarajasingam G, Thanarajasingam U, Ansell SM. Immune Checkpoint Blockade in Lymphoid Malignancies. *FEBS J*. 2016.

Table 1. Comparisons of clinicopathologic characteristics between $CD37^+$ patients and $CD37^-$ patients with DLBCL, GCB-DLBCL, or ABC-DLBCL

Variable	$CD37^+$	$CD37^-$	*P*	$CD37^+$ GCB	$CD37^-$ GCB	*P*	$CD37^+$ ABC	$CD37^-$ ABC	*P*
Patients	212 (100%)	315 (100%)		90 (100%)	178 (100%)		118 (100%)	134 (100%)	**.0023**
Age, years									
< 60	79 (37.3%)	143 (45.4%)	**.064**	42 (46.7%)	89 (50.0%)	.90	34 (28.8%)	52 (38.8%)	**.095**
≥ 60	133 (62.7%)	172 (54.6%)		48 (53.3%)	89 (50.0%)		84 (71.2%)	82 (61.2%)	
Gender									
Female	82 (38.7%)	135 (42.9%)	.34	37 (41.1%)	74 (41.6%)	.94	43 (36.4%)	60 (44.8%)	.18
Male	130 (61.3%)	180 (57.1%)		53 (58.9%)	104 (58.4%)		75 (63.6%)	74 (55.2%)	
Stage									
I/II	105 (51.5%)	138 (45.0%)	.15	53 (61.6%)	88 (50.9%)	.10	49 (43.0%)	48 (36.6%)	.31
III/IV	99 (48.5%)	169 (55.0%)		33 (38.4%)	85 (49.1%)		65 (57.0%)	83 (63.4%)	
B-symptoms									
No	132 (66.7%)	193 (63.3%)	.44	61 (73.5%)	114 (66.7%)	.27	68 (61.3%)	76 (58.0%)	.61
Yes	66 (33.3%)	112 (36.7%)		22 (26.5%)	57 (33.3%)		43 (38.7%)	55 (42.0%)	
LDH level									
Normal	75 (39.1%)	107 (36.8%)	.61	34 (43.6%)	65 (39.6%)	.56	40 (36.4%)	42 (33.9%)	.69
Elevated	117 (60.9%)	184 (63.2%)		44 (56.4%)	99 (60.4%)		70 (63.6%)	82 (66.1%)	
No. of extranodal sites									
0–1	161 (78.2%)	228 (75.7%)	.81	69 (80.2%)	132 (78.1%)	.69	89 (76.7%)	93 (72.1%)	.41
≥ 2	45 (21.8%)	73 (24.3%)		17 (19.8%)	37 (21.9%)		27 (23.3%)	36 (27.9%)	
ECOG performance status									
0–1	175 (89.3%)	220 (79.4%)	**.0044**	74 (92.5%)	126 (81.8%)	**.028**	97 (86.6%)	91 (75.8%)	**.037**
≥ 2	21 (10.7%)	57 (20.6%)		6 (7.5%)	28 (18.2%)		15 (13.4%)	29 (24.2%)	
Size of largest tumor									
< 5cm	98 (60.9%)	131 (56.7%)	.41	45 (67.2%)	73 (55.7%)	.12	50 (54.9%	58 (59.2%)	.56
≥ 5cm	63 (39.1%)	100 (43.3%)		22 (32.8%)	58 (44.3%)		41 (45.1%)	40 (40.8%)	
IPI score									
0–2	132 (67.3%)	173 (61.3%)	.21	64 (78.0%)	106 (66.7%)	.07	64 (58.2%)	64 (53.3%)	.46
3–5	64 (32.7%)	109 (38.7%)		18 (22.0%)	53 (33.3%)		46 (41.8%)	56 (46.7%)	
Therapy response*									
CR	189 (89.2%)	215 (68.3%)	**< .0001**	82 (91.1%)	124 (69.7%)	**< .0001**	103 (87.3%)	89 (66.4%)	**.0001**
PR	18 (8.5%)	52 (16.5%)		6 (6.7%)	25 (14%)		12 (10.2%)	27 (20.1%)	
SD	0 (0%)	23 (7.3%)		0 (0%)	14 (7.9%)		0 (0%)	9 (6.7%)	
PD	5 (2.3%)	25 (7.9%)		2 (2.2%)	15 (8.4%)		3 (2.5%)	9 (6.7%)	
Primary disease									
Extranodal	76 (36.9%)	114 (36.4%)	.91	33 (37.5%)	62 (35.2%)	.72	40 (35.1%)	51 (38.1%)	.63
Nodal	130 (63.1%)	199 (63.6%)		55 (62.5%)	114 (64.8%)		74 (64.9%)	83 (61.9%)	
IgA IHC									
0%	210 (99.1%)	303 (96.2%)	**.045**	89 (98.9%)	171 (96.1%)	.20	117 (99.2%)	129 (96.3%)	.13
100%	2 (0.9%)	12 (3.8%)		1 (1.1%)	7 (3.9%)		1 (0.8%)	5 (3.7%)	
IgG IHC									
0%	189 (89.2%)	283 (89.8%)	.80	82 (91.1%)	159 (89.3%)	.65	103 (87.3%)	121 (90.3%)	.45
100%	23 (10.8%)	32 (10.2%)		8 (8.9%)	19 (10.7%)		15 (12.7%)	13 (9.7%)	
IgM IHC									
Negative	142 (67.0%)	239 (75.9%)	**.025**	76 (84.4%)	154 (86.5%)	.65	63 (52.9%)	82 (61.2%)	.19
Positive	70 (33.0%)	76 (24.1%)		14 (15.6%)	24 (13.5%)		56 (47.1%)	52 (38.8%)	

LDH, lactate dehydrogenase; ECOG, Eastern Cooperative Oncology Group; CR, complete remission; PR, partial response; SD, stable disease; PD, progressive disease; IHC, immunohistochemistry.

*We calculated *P* values as CR *vs.* other responses. Clinicopathologic data were not available for some cases due to clinical data unavailability and tissue exhaustion.

Table 2. Differential expression of tetraspanins and B-cell receptor signaling-related genes between CD37⁻ and CD37⁺ patients with GCB- or ABC-DLBCL

	CD37⁻ *vs.* CD37⁺ in GCB/ABC DLBCL		
Genes	Downregulation in CD37⁻	*Genes*	Upregulation in CD37⁻
CD37	↓ in both GCB ($P = .036$) and ABC ($P < .0001$)	***CD63***	↑ in ABC ($P < .0001$)
CD20	↓ in both GCB ($P = .0008$) and ABC ($P = .0009$)	***MS4A4A* (*CD20L1*)**	↑ in both GCB ($P = .0073$) and ABC ($P = .059$)
CD79A	↓ in both GCB ($P = .002$) and ABC ($P = .009$)	***MS4A6A* (*CD20L3*)**	Trend of ↑ in ABC ($P = .057$)
CD79B	↓ in ABC ($P = .032$)	***AKT1***	↑ in GCB ($P = .019$)
CD22	↓ in both GCB ($P = .016$) and ABC ($P = .011$)		
CD23	↓ in GCB ($P = .016$)		
STAP1	↓ in GCB ($P = .0012$)		
SWAP70	↓ in GCB ($P = .0036$)		
SYK	↓ in ABC ($P = .045$)		
CARD11	↓ in ABC ($P = .05$)		
BCL10	Trend of ↓ in ABC ($P = .07$)		
MALT1	↓ in GCB ($P = .021$)		
CD40	↓ in GCB ($P = .016$)		
BLNK	Trend of ↓ in ABC ($P = .064$)		
MYC	Trend of ↓ in ABC ($P = .08$)		
REL	↓ in GCB ($P = .0031$)		
PIK3C2B	↓ in GCB ($P = .046$) and ABC ($P = .07$)		
A20/TNFAIP3	↓ in GCB ($P = .018$)	***A20/TNFAIP3***	↑ in ABC ($P = .036$)

The *P* values were obtained by unpaired *t* test (2-tailed).

Table 3. Multivariate survival analysis for CD37 expression adjusting clinical factors and molecular biomarkers associated with CD37$^{+/-}$ in overall DLBCL, GCB-DLBCL, and ABC-DLBCL, and multivariate analysis in CD37^{+} GCB-DLBCL

	Overall Survival			Progression-free survival		
	HR	**95% CI**	***P***	**HR**	**95% CI**	***P***
In overall DLBCL						
Female sex	0.67	0.42-1.07	0.09	0.74	0.48-1.15	0.18
B-symptoms	1.68	1.04-2.73	**0.035**	1.69	1.06-2.68	**0.026**
Tumor size ≥5cm	1.32	0.83-2.09	0.24	1.27	0.82-1.96	0.28
IPI >2	2.35	1.49-3.70	**< 0.001**	2.43	1.57-3.75	**< 0.001**
ABC subtype	2.12	1.24-3.60	**0.006**	1.79	1.08-2.98	**0.025**
TP53 mutation	1.76	1.05-2.96	**0.033**	1.68	1.02-2.75	**0.040**
p63^{+}	0.71	0.47-1.07	0.097	0.81	0.55-1.19	0.29
p50^{high}	1.09	0.70-1.71	0.70	1.13	0.73-1.74	0.58
CXCR4^{high}	1.81	1.06-3.10	**0.03**	2.15	1.28-3.63	**0.004**
‡CD37^{+}	**0.29**	**0.17-0.51**	**< 0.001**	**0.26**	**0.15-0.44**	**< 0.001**
CD37^{-}	**3.43**	**1.96-6.02**	**< 0.001**	**3.91**	**2.28-6.71**	**< 0.001**
In GCB-DLBCL						
Female sex	0.51	0.26-1.01	**0.053**	0.57	0.31-1.06	0.075
B-symptoms	1.27	0.67-2.42	0.46	1.16	0.65-2.10	0.61
Tumor size ≥5cm	1.65	0.88-3.08	0.12	1.61	0.91-2.86	0.10
IPI >2	3.66	1.90-7.01	**< 0.001**	3.39	1.90-6.06	**< 0.001**
TP53 mutation	1.36	0.64-2.89	0.42	1.40	0.70-2.79	0.35
p50^{high}	0.77	0.35-1.69	0.51	0.71	0.33-1.57	0.40
p65^{high}	1.90	0.81-4.46	0.14	1.48	0.65-3.36	0.35
p-STAT3^{high}	0.73	0.28-1.89	0.51	1.20	0.54-2.69	0.65
MYC–R^{+}	3.01	1.06-3.98	**0.038**	2.46	1.03-3.04	**0.043**
*Myc^{high}	2.18	1.14-4.16	**0.018**	1.67	0.90-3.08	0.10
‡CD37^{+}	**0.21**	**0.078-0.54**	**0.001**	**0.18**	**0.073-0.43**	**< 0.001**
CD37^{-}	**4.86**	**1.84-12.82**	**0.001**	**5.64**	**2.32-13.74**	**< 0.001**
In ABC-DLBCL						
Female sex	0.86	0.51-1.46	0.58	0.94	0.57-1.55	0.80
B-symptoms	1.57	0.93-2.66	0.098	1.52	0.91-2.54	0.11
Tumor size ≥5cm	1.31	0.77-2.24	0.12	1.18	0.71-1.94	0.53
IPI >2	2.75	1.65-4.56	**< 0.001**	2.76	1.58-4.82	**< 0.001**
p50^{high}	1.87	1.10-3.16	**0.02**	1.73	1.07-2.81	**0.027**
survivin^{high}	1.61	0.89-2.88	0.11	1.47	0.85-2.55	0.17
CXCR4^{high}	2.17	1.30-3.61	**0.003**	1.90	1.11-3.24	**0.019**
p63^{+}	0.58	0.34-1.00	**0.049**	0.62	0.38-1.00	**0.048**
‡CD37^{+}	**0.39**	**0.23-0.67**	**0.001**	**0.40**	**0.23-0.67**	**0.001**
CD37^{-}	**2.57**	**1.50-4.40**	**0.001**	**2.53**	**1.50-4.44**	**0.001**
In CD37^{+} GCB-DLBCL						
Female sex	0.25	0.016-4.08	0.33	0.17	0.014-2.07	0.17
B-symptoms	2.13	0.17-27.3	0.56	1.59	0.14-17.9	0.71
Tumor size ≥5cm	2.61	0.31-22.2	0.38	1.44	0.24-8.62	0.69
IPI >2	2.08	0.14-30.5	0.60	2.01	0.14-28.0	0.60
TP53 mutation	1.37	0.095-19.8	0.82	3.17	0.35-28.8	0.31
Myc^{high}	20.0	1.87-213.6	**0.013**	14.1	1.39-143	**0.025**
CXCR4^{high}	5.45	0.61-48.7	0.13	6.65	0.85-51.8	0.071

HR, hazard ratio; CI, confidence interval. The cutoffs for high/positive expression of p50, p65, p-STAT3, Myc, CXCR4, survivin, and p63 were ≥20%, ≥50%, ≥50%, ≥70%, ≥20%, >25%, and >5%, respectively.

* Two different Cox regression models were used to include either *MYC*–R^+ or Myc^{high} as one variant separately. *MYC* rearrangement was not included as a variant in the multivariate analysis in $CD37^+$ GCB-DLBCL because of limited case numbers.

_ Two different models were used to include either $CD37^+$ or $CD37^-$ as one variant separately.

Table 4. Gene expression profiling analysis between CD37^{+} and CD37^{-} DLBCL groups

Function categories	Upregulated	Downregulated
	CD37^{-} *vs.* CD37^{+} DLBCL (FDR < 0.05)	
Immune responses, inflammation, host defense	*FCGR1B* ↑ *LILRB2* ↑ *SERPING1* ↑ *IRF1* ↑ *TLR2* ↑ *SAMHD1* ↑ *IFITM1* ↑ *IFITM3* ↑ *PYCARD* ↑ *HEBP1* ↑	
Signaling	*FNIP2* ↑ *RCAN1* ↑ *SERPINA1* ↑	*CD37* ↓ *MS4A1/CD20* ↓ *VSNL1* ↓ *LPAR6* ↓
Differentiation	*FNDC3B* ↑	*AICDA* ↓ *BCL11A* ↓ *FOXP1* ↓ *XBP1* ↓ *PAX5* ↓
Gene expression, translation, cell cycle	*EIF1* ↑	*CDK5R1* ↓ *METTL2A/B* ↓ *ZNF581* ↓ *ZNF765* ↓
Apoptosis, DNA damage response	*DRAM1* ↑	*C9orf102* ↓
Metabolism, protein repair and degradation, oxidative stress, lipid movement, transport, intracellular membrane trafficking	*GCH1* ↑ *MT1G* ↑ *MT1P2* ↑ *PAM* ↑ *MT1E* ↑ *C11orf67* ↑ *MT1E/MT1H/MT1M* ↑ *UBR1* ↑ *APOL6* ↑ *RCN1* ↑ *PCMT1* ↑ *MSRB2* ↑ *NUB1* ↑ *RAB6A* ↑ *ARF4* ↑ *RAB1B* ↑ *AQP9* ↑ *CDIPT* ↑ *C12orf62* ↑ *DPYD* ↑	*ZDHHC21* ↓ *GOLGA8A/B* ↓
Adhesion, regulation of actin, cytoskeleton, exocytosis, and extracellular matrix	*RAB27A* ↑ *AOC3* ↑ *GPR124* ↑ *NINJ1* ↑ *WDR1* ↑ *CRISPLD2* ↑ *RHOU* ↑	*DMD* ↓
Unknown function, RNA gene	*ANKRD22* ↑ *MOP-1* ↑ *CNIH4* ↑ *PLEKHO2* ↑ *FTHP1* ↑ *C4orf32* ↑ *FAM167B* ↑ *PWWP2B* ↑	*FAM129C* ↓ *NAPSB* ↓ *SNORA74A* ↓ *BRWD2* ↓ *FAM108C1* ↓ *LOC283887* ↓ *RAB7L1* ↓ *LOC133874* ↓
	CD37^{-} *vs.* CD37^{+} ABC-DLBCL (FDR < 0.05)	
Immune responses, inflammation, host defense	*LILRB2* ↑ *C1S* ↑ *AIF1* ↑ *IFITM1* ↑ *IFITM3* ↑ *SERPING1* ↑ *HLA-C* ↑ *LST1* ↑ *B2M* ↑ *ISG15* ↑	
Signaling	*SRC* ↑ *STAT4* ↑ *CD63* ↑ *SEMA4D* ↑ *SECTM1* ↑ *VDR* ↑ *RCAN1* ↑ *ACVRL1* ↑ *PREX1* ↑ *PROCR* ↑ *TNIP2* ↑ *RALB* ↑	*CD37* ↓
Differentiation		*AICDA* ↓ *BCL11A* ↓ *FOXP1* ↓ *IKZF1* ↓ *PAX5* ↓
Gene expression, translation	*TCF7L2* ↑ *EIF4E3* ↑ *EIF1* ↑ *C14orf4* ↑ *KLF3* ↑	*TBL1XR1* ↓ *HELLS* ↓ *RPS2* ↓ *EBF1* ↓ *ZNF587* ↓
Apoptosis, autophagy, DNA repair	*DRAM1* ↑ *C19orf40* ↑	*C9orf102* ↓
Metabolism, ion channel, transport, trafficking, protein degradation	*FAM26F* ↑ *GCH1* ↑ *MT1P2* ↑ *MT1E* ↑ *STOM* ↑ *MT1E/MT1H/MT1M* ↑ *ACSL1* ↑ *AAK1* ↑ *VAMP5* ↑ *RAB13* ↑ *RCN1* ↑ *RNF217* ↑ *RAB6A* ↑ *MGST2* ↑ *BLVRA* ↑ *C14orf133* ↑ *PDXK* ↑ *GMPPA* ↑ *HTATIP2* ↑ *HEBP1* ↑ *CHP1* ↑	*C7orf68* ↓ *GOLGA8B* ↓ *RIMKLB* ↓ *DPY19L2* ↓ *UBE3C* ↓ *DNAJB7* ↓
Adhesion, regulation of actin, cytoskeleton, exocytosis, and extracellular matrix	*RAB27A* ↑ *PECAM1* ↑ *RHOU* ↑ *MYOF* ↑ *DYSF* ↑ *CCDC80* ↑ *AOC3* ↑ *CTNNA1* ↑ *GPR124* ↑	*RALGPS2* ↓
Unknown function, RNA gene	*ANKRD22* ↑ *GLIPR2* ↑ *NKG7* ↑ *CNIH4* ↑ *SAMD3* ↑ *TMEM176A* ↑ *SLFN12* ↑ *PLEKHO2* ↑ *C21orf33/PWP2* ↑	*FAM129C* ↓ *C13orf18* ↓ *NAPSB* ↓ *SNORA68* ↓ *SNORA74A* ↓ *BRWD2* ↓ *FAM108C1* ↓ *SNORD104* ↓ *FLJ43663* ↓ *SNHG12* ↓ *PMS2L1* ↓ *LOC284513* ↓
	PI3K^{high}/CD37^{-} *vs.* PI3K^{high}/CD37^{+} ABC-DLBCL (FDR < 0.01)	
Immune responses, inflammation, host defense	*FCGR1B* ↑ *GBP1* ↑ *FPR2* ↑ *TRBC1* ↑ *IFITM1* ↑ *FCGR3B* ↑ *FCGR1A/C* ↑ *C3AR1* ↑ *CD14* ↑	
Signaling	*SECTM1* ↑ *TNFSF10* ↑ *SEMA4D* ↑ *APLP2* ↑	
Differentiation, transcription factors	*BCL11B* ↑ *KLF3* ↑	
Cell cycle	*CCND1* ↑ *PTP4A2* ↑	
Apoptosis	*DRAM1* ↑ *EPB41L3* ↑	
Ion channel, transport, trafficking, protein degradation, metabolism	*MT1H* ↑ *FAM26F* ↑ *MT1G* ↑ *MT2A* ↑ *MT1X* ↑ *CPD* ↑ *MT1E/MT1H/MT1M* ↑ *SLC8A1* ↑ *MT1E* ↑ *AAK1* ↑ *LYST* ↑ *APOL6* ↑ *RAB1A* ↑	
Adhesion	*PECAM1* ↑	
RNA regulation, unknown function	*ANKRD22* ↑ *ZC3H12C* ↑ *GLIPR2* ↑	*SNORD104* ↓
	CD37^{-} ABC *vs.* CD37^{-} GCB (FDR < 0.01, fold change >2)	
Immune responses, inflammation	*TNFRSF13B* ↑ *S100A8* ↑ *GZMB* ↑ *CLECL1* ↑ *LILRB2* ↑ *FCRL5* ↑ *CCL8* ↑	*IGHG1* ↓

Signaling	*IGHM* ↑	*MME* ↓ *STAP1* ↓
Transcription regulation, DNA replication, microRNA	*BATF* ↑ *IRF4* ↑ *MIR155HG* ↑	*MYBL1* ↓ *ELL3/SERINC4* ↓ *STAG3* ↓ *SSBP2* ↓ *BCL6* ↓
Metabolism, ion channel	*FUT8* ↑ *FAM26F* ↑ *DHRS9* ↑	
Adhesion, cytoskeleton, extracellular matrix	*TUBB4* ↑ *CD44* ↑	*CILP* ↓ *KANK1* ↓ *PCDHGB7* ↓ *MARCKSL1* ↓
Unknown function	*ANKRD22* ↑ *C1orf186* ↑*C13orf18* ↑ *MPEG1* ↑	*FLJ42418* ↓ *C17orf99* ↓ *TMEM108* ↓ *TEX9* ↓ *CRNDE* ↓ *CCDC85A* ↓ *BTNL9* ↓ *KIAA0746* ↓
	CD37$^+$ ABC *vs.* CD37$^+$ GCB (FDR < 0.01, fold change >2.18)	
Immune responses	*TNFRSF13B* ↑ *CLECL1* ↑ *FCRL5* ↑ *GZMB* ↑	*IGHG1* ↓ *HLA-DOB* ↓ *LRMP* ↓ *CXCL14* ↓
Signaling	*IGHM* ↑ *BLNK* ↑	*MME* ↓ *STAP1* ↓ *PTPRS* ↓ *SPRED2* ↓ *PDE4D* ↓ *RRAS2* ↓ *FNDC1* ↓
Differentiation	*AICDA* ↑	*LMO2* ↓
Transcription regulation, DNA replication, microRNA	*FOXP1* ↑ *PARP15* ↑ *BATF* ↑ *TCF4* ↑ *IRF4* ↑ *MIR155HG* ↑	*MYBL1* ↓ *STAG3* ↓ *HOPX* ↓*TOX* ↓ *SSBP2* ↓ *REL* ↓
Cell cycle		*NEK6* ↓
Metabolism, transport	*XK* ↑ *P2RX5* ↑ *FUT8* ↑ *SLC2A13* ↑	*SLC12A8* ↓ *PLEKHF2* ↓ *GALNT14* ↓ *SULF1* ↓ *LHPP* ↓
Adhesion, cytoskeleton, extracellular matrix, migration	*TUBB4* ↑	*CILP* ↓ *POSTN* ↓ *MARCKSL1* ↓ *DPT* ↓ *PCDHGB7* ↓ *RAPH1* ↓ *CPNE3* ↓ *COL5A1* ↓ *KANK1* ↓ *PTK2* ↓
Unknown function	*C13orf18* ↑ *FAM129C* ↑ *C1orf186* ↑ *TBC1D27* ↑ *MPEG1* ↑	*C17orf99* ↓ *FLJ42418* ↓ *CCDC144B* ↓ *TMEM108* ↓ *BTNL9* ↓ *PRO1483* ↓ *CCDC85A* ↓ *KIAA0746* ↓

FDR, false discovery rate.

Table 5. Differential expression of genes involved in immune responses or differentiation between $CD37^-$ and $CD37^+$ patients, between $p50^{high}/CD37^-$ and $p50^{low}/CD37^-$ patients ($CD37^-$ was associated with $p50^{high}$), between $CXCR4^{high}/CD37^+$ and $CXCR4^{low}/CD37^+$ patients ($CD37^+$ was associated with $CXCR4^{high}$ in ABC-DLBCL), and between $CD37^+$ ABC-DLBCL and $CD37^+$ GCB-DLBCL ($CD37^+$ was associated with ABC cell-of-origin)

	$CD37^-$ *vs.* $CD37^+$ in GCB/ABC DLBCL	$p50^{high}$ *vs.* $p50^{low}$ in $CD37^-$ GCB/ABC DLBCL	$CXCR4^{high}$ *vs.* $CXCR4^{low}$ in $CD37^+$ GCB/ABC DLBCL	ABC *vs.* GCB in $CD37^+$ DLBCL
Genes involved in immune responses or differentiation				
ICOSLG	↓ in GCB ($P = .0036$)			↓ ($P < .0001$)
CD58	↓ in GCB ($P = .022$)		↓ in $CD37^+$ ABC ($P = .056$)	↓ ($P = .0009$)
***FCGR2A* (*CD32A*)**	↑ in both GCB ($P = .016$) and ABC ($P = .044$)	↑ in both $CD37^-$ GCB ($P = .0078$) and $CD37^-$ ABC ($P = .016$)	↓ in $CD37^+$ ABC ($P = .02$)	↑ ($P = .0022$)
***FCGR1B* (*CD64*)**	↑ in both GCB ($P = .01$) and ABC ($P = .0007$)	↑ in both $CD37^-$ GCB ($P = .0003$) and $CD37^-$ ABC ($P = .0094$)		↑ ($P = .0005$)
C1QB	↑ in both GCB ($P = .0001$) and ABC ($P = .0027$)	↑ in both $CD37^-$ GCB ($P < .0001$) and $CD37^-$ ABC ($P = .0007$)		↑ ($P < .0001$)
CD8A	↑ in ABC ($P = .0014$)	↑ in both $CD37^-$ GCB ($P = .017$) and $CD37^-$ ABC ($P = .039$)		
CD8B	↑ in both GCB ($P = .068$) and in ABC ($P = .0012$)	↑ in both $CD37^-$ GCB ($P = .0059$) and $CD37^-$ ABC ($P = .038$)	Trend of ↓ in $CD37^+$ GCB ($P = .08$) and $CD37^+$ ABC ($P = .068$)	
***PDCD1* (*PD-1*)**	↑ in ABC ($P = .03$); ↑ in $p50^{nigh}$ GCB ($P = .05$)	↑ in $CD37^-$ ABC ($P = .03$)	↓ in $CD37^+$ GCB ($P = .014$) and trend of ↓ in $CD37^+$ ABC ($P = .069$)	
***CD274* (*PD-L1*)**		↑ in $CD37^-$ GCB ($P = .013$)	↑ in $CD37^+$ ABC ($P = .018$)	
***PDCD1LG2* (*PD-L2*)**	Trend of ↑ in ABC ($P = .09$)	↑ in $CD37^-$ GCB ($P = .0025$)		
CTLA4		↑ in both $CD37^-$ GCB ($P = .027$) and $CD37^-$ ABC ($P = .0032$)	↓ in $CD37^+$ ABC ($P = .0005$) trend of ↓ in $CD37^+$ GCB ($P = .086$)	
***HAVCR2* (*TIM3*)**		↑ in both $CD37^-$ GCB ($P = .0027$) and $CD37^-$ ABC ($P = .0001$)		
CIITA	↓ in GCB ($P = .014$)			↓ ($P < .0001$)
HLA-A-G	(↑ in the overall $CD37^-$ *vs.* $CD37^+$ ABC, but it is due to the association with p50 and CXCR4)	↑ in both $CD37^-$ GCB ($P = .0056$) and $CD37^-$ ABC ($P = .0003$)	↓ in both $CD37^+$ GCB ($P = .0073$) and $CD37^+$ ABC ($P = .025$)	
***LILRB2* (*LIR2*)**	↑ in both GCB ($P = .0014$) and ABC ($P < .0001$)	↑ in both $CD37^-$ GCB ($P = .0001$) and $CD37^-$ ABC ($P = .0065$)	↓ in $CD37^+$ GCB ($P = .0017$)	↑ ($P < .0001$)
***LILRA3* (*LIR4*)**	↑ in ABC ($P = .0021$)	↑ in $CD37^-$ GCB ($P = .001$)		↑ ($P = .0028$)
***LILRA1* (*LIR6*)**	↑ in GCB ($P = .028$)	↑ in $CD37^-$ GCB ($P = .0062$)		↑ ($P = .0002$)
CASP1	↑ in ABC ($P = .018$)	↑ in both $CD37^-$ GCB ($P = .041$) and $CD37^-$ ABC ($P = .029$)	↓ in $CD37^+$ ABC ($P = .0056$)	↑ ($P = .023$)
CASP7	↑ in GCB ($P = .02$)	↑ in $CD37^-$ ABC ($P = .031$)		↑ ($P < .0001$)
CASP8	↑ in GCB ($P = .023$)			↑ ($P < .0001$)
CASP10	↑ in ABC ($P = .018$); trends of ↑ in GCB ($P = .068$)		↓ in $CD37^+$ GCB ($P = .0097$)	
CXCL12	↑ in ABC ($P = .0072$)	↑ in both $CD37^-$ GCB ($P = .025$) and $CD37^-$ ABC ($P = .0007$)	↓ in $CD37^+$ ABC ($P = .0002$)	
IL6R		↑ in both $CD37^-$ GCB ($P = .009$) and $CD37^-$ ABC ($P = .0001$)	↓ in $CD37^+$ ABC ($P = .049$)	
IL10RB	↑ in ABC ($P = .038$)	↑ in $CD37^-$ GCB ($P = .0005$)	↑ in $CD37^+$ ABC ($P = .034$)	
IL21R	↓ in GCB ($P = .0036$)			
IRF1	↑ in both GCB ($P = .025$) and ABC ($P = .0005$)	↑ in $CD37^-$ ABC ($P = .0004$)		↑ ($P = .044$)
STAT1	↑ in ABC ($P = .017$)	↑ in both $CD37^-$ GCB ($P = .0068$) and $CD37^-$ ABC ($P = .0006$)		
IFIT3	↑ in both GCB ($P = .0071$) and ABC ($P = .0011$)	↑ in $CD37^-$ GCB ($P < .0001$)	↓ in $CD37^+$ GCB ($P = .047$)	↑ ($P = .011$)
CARD16	↑ in ABC ($P = .0022$)		↓ in $CD37^+$ ABC ($P = .022$)	
TCL1A	↓ in ABC ($P = .0071$)	Trend of ↓ in $CD37^-$ ABC ($P = .076$)	↑ in $CD37^+$ GCB ($P = .036$)	
AICDA	↓ in ABC ($P < .0001$)		↑ in both $CD37^+$ GCB ($P = .028$) and $CD37^+$ ABC ($P < .0001$)	↑ ($P < .0001$)
FOXP1	↓ in ABC ($P < .0001$)		↑ in $CD37^+$ GCB ($P = .03$)	↑ ($P < .0001$)
BCL11A	↓ in both GCB ($P = .0017$) and ABC ($P < .0001$)	↓ in both $CD37^-$ GCB ($P = .0058$) and $CD37^-$ ABC ($P = .017$)	↑ in both $CD37^+$ GCB ($P = .04$) and $CD37^+$ ABC ($P = .0006$)	
LMO2	↓ in GCB ($P = .0007$)			↓ ($P < .0001$)
***POU2F2* (*OTF2*)**	↓ in ABC ($P = .0001$)			↑ ($P < .0001$)

* The cutoffs for $p50^{high}$ and $CXCR4^{high}$ were ≥20%. The *P* values were obtained by unpaired *t* test (2-tailed).

Figure Legends

Figure 1. Expression and prognostic effect of CD37 antigen in patients with DLBCL. (A-B) Representative CD37 negative and positive (red) immunohistochemistry results (60×). Cell nuclei were counterstained with hematoxylin (blue). Images were obtained with an Olympus AX70 microscope with a DP71 camera. (C) Histogram of CD37 immunohistochemistry scores in the DLBCL discovery cohort. (D) A scatter plot for CD37 expression in DLBCL and comparison between GCB and ABC cell-of-origin. (E) Patients with $CD37^-$ DLBCL had significantly worse OS and PFS compared with patients with $CD37^+$ DLBCL, with a HR of 2.80 and 95% CI of 1.95-3.38 for OS, and a HR of 2.89 and 95% CI of 2.07-3.45 for PFS. (F-H) The adverse prognostic effect of CD37 loss was independent of GCB and ABC cell-of-origin, high and low IPI scores, and primary nodal (NL) and primary extranodal (ENL) origin.

Figure 2. CD37 and CD20 expression show correlations but the prognostic significance of CD37 is independent of CD20 expression in DLBCL. (A) In both GCB- and ABC-DLBCL, the $CD37^-$ group had significantly lower mean levels of *CD37* and *CD20* mRNA expression compared with the $CD37^+$ group. (B) Geometric mean fluorescence intensities (gMFI) of CD37 and CD20 protein expression in 3 different $CD37^-$ and 3 different $CD37^+$ DLBCL cell lines measured by flow cytometry. CD20 expression on the plasma membrane of DLBCL cells were detected by a non-therpeutic CD20 antibody (2H7, BioLegend) (left), and by therapeutic Rutuxan (Roche) (right). Results are representative for 2 independent experiments. Coefficient for linear regression: R^2 = 0.9737 (Left) and R^2 = 0.8043 (right). Dotted lines show 95% confidence interval. (C) Low *CD20* mRNA expression (< mean) correlated with significantly worse OS and PFS, especially in ABC-DLBCL. (D) However, $CD37^+$ patients with lower *CD20* mRNA levels had significantly better OS and PFS than $CD37^-$ patients with higher *CD20* mRNA levels. (E) In GCB-DLBCL, CD37 antigen status but not *CD20* mRNA levels predicted survival.

In ABC-DLBCL, CD37 status and *CD20* mRNA levels showed prognostic impact independent of each other, but CD37 status showed stronger prognostic impact. (F) In an independent CHOP-treated DLBCL cohort, overall $CD37^+$ patients had significantly better PFS than $CD37^-$ patients. However, the favorable impact was limited in patients with low (≤50%) CD37 levels and patients with high (>50%) CD37 expression showed similar PFS with $CD37^-$ patients.

Figure 3. Correlation analysis and the robust prognostic effect of CD37 expression in patients with DLBCL. (A) A distribution plot showing that $CD37^-$ GCB-DLBCL (denoted by the yellow bar) more frequently had *TP53* mutations (highlighted in red) or high levels of nuclear p50 (yellow), Myc (green), phosphorylated STAT3 (orange) and p65 (lighter red) expression compared with $CD37^+$ GCB-DLBCL (denoted by the blue bar). (B) A distribution plot showing that $CD37^-$ ABC-DLBCL more frequently had high nuclear p50 (yellow) and survivin (pink) expression and *BCL6* translocation (green), whereas $CD37^+$ ABC-DLBCL more frequently had PI3K (blue) and CXCR4 (purple) overexpression. Each column in parts A and B represents one patient; cases without indicated abnormalities detected are shown in light blue (negative) or white (unknown). (C) In GCB-DLBCL, CD37 positivity predicted significantly improved survival, regardless of presence of *TP53* mutations, $p50^{high}$, Myc^{high}, $p\text{-}STAT3^{high}$, $GCET1^{high}$, and to less extent, *MYC* translocations. Conversely, the adverse effect of CD37 negativity was independent of all these biomarkers. Particularly, $CD37^-$ patients without *TP53* mutations and p50/Myc overexpression remained to have significantly worse survival than patients with $CD37^+$ GCB-DLBCL. (D) In GCB-DLBCL, CD37 positivity predicted significantly better survival even when the patients had high IPI scores. (E) In ABC-DLBCL, the adverse prognostic effect of CD37 negativity was independent of p50, survivin, p63, PI3K, and CXCR4 expression and *BCL6* translocations. In particular, $CD37^-$ patients without p50 and survivin overexpression remained to have significantly worse survival than patients with $CD37^+$ ABC-DLBCL. (F) In ABC-DLBCL,

CD37 and IPI had independent prognostic impact. The cutoffs for high/positive expression as indicated by $p50^+$, Myc^+, $p\text{-}STAT3^+$, $GCET1^+$, $survivin^+$, $p63^+$, $PI3K^+$, and $CXCR4^+$ in the figures were ≥20%, ≥70%, ≥50%, ≥50%, >25%, >5%, ≥70%, and ≥20%, respectively.

Figure 4. Comparison of risk stratification in patients with DLBCL by the traditional IPI and adjusted IPI scores. (A) Risk stratification of DLBCL groups by the traditional IPI. (B) Risk stratification of DLBCL by the molecularly adjusted IPI for R-CHOP ("M-IPI-R"), defined by each patient's IPI score plus risk scores for CD37 status ($CD37^+$: 0; $CD37^-$: 1 or 2 as indicated) and GCB/ABC cell-of-origin (GCB: 0; ABC: 1). (C) Risk stratification of DLBCL by the IPI plus immunohistochemistry ("IPI+IHC"), defined by each patient's IPI score plus risk scores for CD37 status ($CD37^+$: 0; $CD37^-$: 3), and Myc and Bcl-2 protein levels (low [IHC <70%]: 0; high [IHC ≥70%]: 1).

Figure 5. Gene expression profiling (GEP) analysis in DLBCL. (A) Heatmap for GEP comparison between $CD37^+$ and $CD37^-$ DLBCL (FDR <0.05). (B) The KEGG chemokine signaling pathway gene set was enriched in the $CD37^-$ DLBCL group with an enrichment score of 0.45 (FDR: 0.09). (C) The KEGG phagosome gene set was enriched in $CD37^-$ ABC-DLBCL with an enrichment score of 0.55 (FDR: 0.006). (D) Heatmap for GEP comparison between $CD37^+$ ABC-DLBCL and $CD37^-$ ABC-DLBCL groups with high (≥70%) PI3K expression (FDR <0.01). (E) Heatmap for genes differentially expressed between GCB and ABC subtypes of $CD37^-$ DLBCL with >2 fold difference (FDR <0.01). (F) Heatmap for genes differentially expressed between GCB and ABC subtypes of $CD37^+$ DLBCL with >2.4 fold difference (FDR <0.01).

Figure 6. Comparison of *ICOSL*, *PDCD1*, and PD-1 expression in CD37$^+$ and CD37$^-$ DLBCL. (A) CD37 positivity was associated with significantly higher levels of *ICOSLG* in GCB-DLBCL. (B) CD37 loss correlated with *PDCD1* (*PD-1*) upregulation in ABC-DLBCL. (C) In p50^{high} (≥20% nuclear expression) DLBCL, CD37 loss correlated with *PD-1* upregulation in both GCB- and ABC-DLBCL. (D-E) CD37 loss in DLBCL correlated with significantly higher levels of PD-1 receptor expression on both cytotoxic and helper T cells. (F) The ABC subtype had significantly higher *CD274* (*PD-L1*) levels compared with the GCB subtype, which was more apparent in the CD37$^-$ DLBCL subset.

Figure 7. A hypothetic model illustrating the pivotal role of CD37 status for R-CHOP outcome in DLBCL and the important molecular mechanisms for R-CHOP resistance in CD37$^-$ DLBCL and CD37$^+$ ABC-DLBCL.

(I) CD37 positivity independently predicted favorable outcome, likely because CD37$^+$ DLBCL is sensitive to R-CHOP owing to increased *CD20* and *ICOSLG* whereas decreased PD-1 expression (depicted by green □, □, and □, respectively), as well as CD20-independent CD37 function in enhancing antibody-dependent cellular cytotoxicity (ADCC) and apoptosis upon CD20-rituximab ligation (*). This favorable impact can be hindered by *ICOSLG* and *MHC-II* downregulation, upregulation of *PD-L1*, *AICDA*, *LILRA/B*, *IL10*/*IL10RA*, and antiapoptotic pathways downstream of the chronic active B-cell receptor (BCR) signaling in ABC-DLBCL.

(II) CD37 loss robustly predicted poor survival. Rituximab efficacy is limited due to decreased CD20 levels (depicted by yellow □, with postulated reasons of attenuated BCR, cytokine, and trogocytosis) and loss of CD37-rituximab signaling. The worse prognosis is also contributed by increased PD-1 (highlighted by yellow □), *ICOSLG* downregulation (highlighted by yellow □), and frequent *TP53* mutations, Myc, STAT3, or p50 overexpression in CD37$^-$ DLBCL (which were probably oncogenic drivers acquired during lymphomagenesis and further escaped from

immune surveillance by various mechanisms as depicted). Illustrated immune escape mechanisms includes upregulation of *PD-L1*/*L2*, *LILRB/A*, *TIM3*, *CTLA4*, and the IL6/IL10 pathway, and downregulation of *MHC-I*/*II*, *CIITA*, and costimulatory molecules *CD58* and *CD40*. The model is based on our biomarker correlation, GEP, and survival analysis, except the speculated CD37 functions during R-CHOP treatment as denoted by "*".

Fig. 1

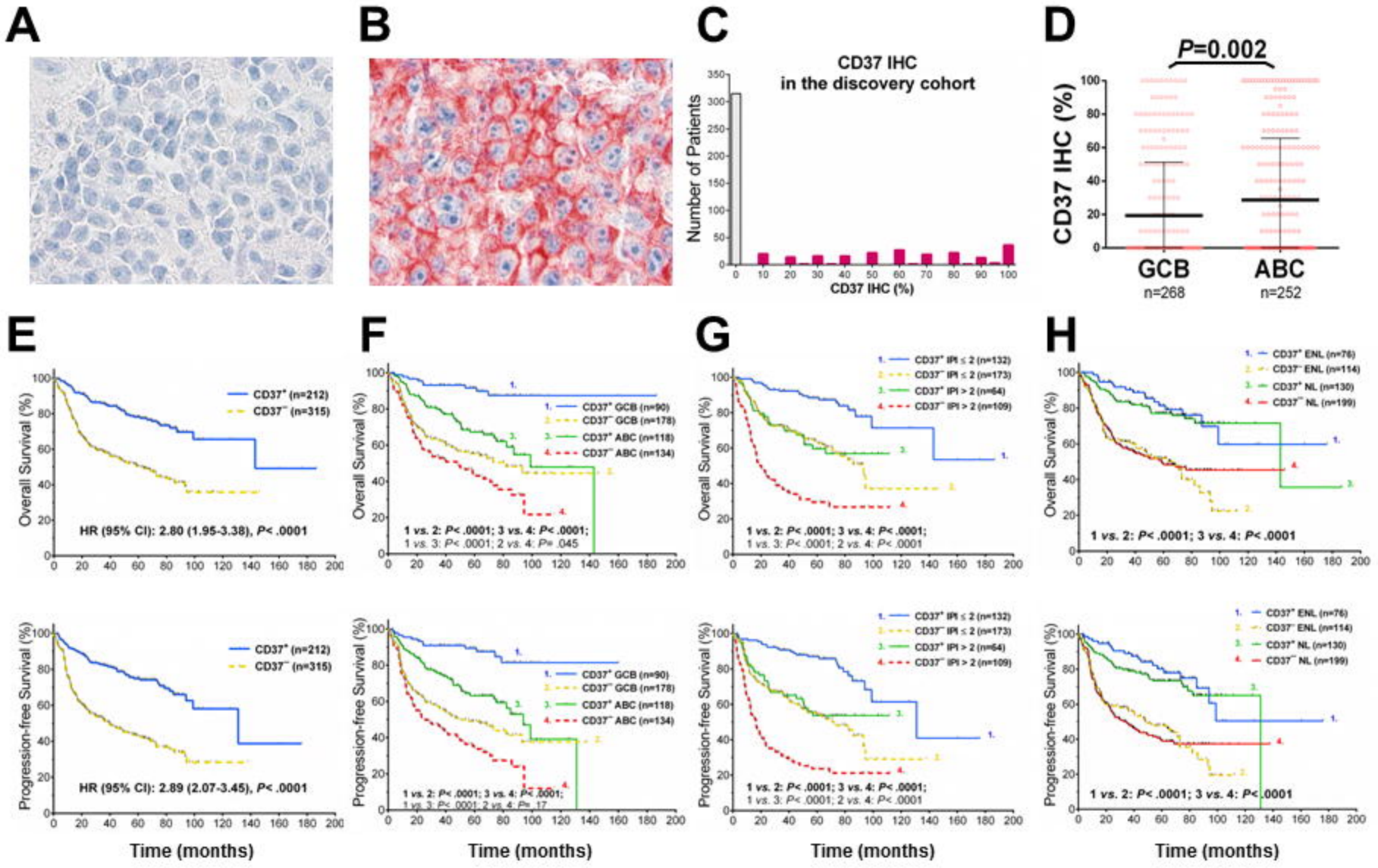
A
B
C
CD37 IHC
in the discovery cohort
Number of Patients
CD37 IHC (%)
D
P=0.002
CD37 IHC (%)
GCB
n=268
ABC
n=252
E
F
G
H
Overall Survival (%)
Progression-free Survival (%)
CD37+ (n=212)
CD37− (n=315)
HR (95% CI): 2.80 (1.95-3.38), P< .0001
HR (95% CI): 2.89 (2.07-3.45), P< .0001
CD37+ GCB (n=90)
CD37− GCB (n=178)
CD37+ ABC (n=118)
CD37− ABC (n=134)
1 vs. 2: P< .0001; 3 vs. 4: P< .0001;
1 vs. 3: P< .0001; 2 vs. 4: P= .045
1 vs. 2: P< .0001; 3 vs. 4: P< .0001;
1 vs. 3: P< .0001; 2 vs. 4: P< .0001
CD37+ IPI ≤ 2 (n=132)
CD37− IPI ≤ 2 (n=173)
CD37+ IPI > 2 (n=64)
CD37− IPI > 2 (n=109)
CD37+ ENL (n=76)
CD37− ENL (n=114)
CD37+ NL (n=130)
CD37− NL (n=199)
1 vs. 2: P< .0001; 3 vs. 4: P< .0001
Time (months)

Fig. 2

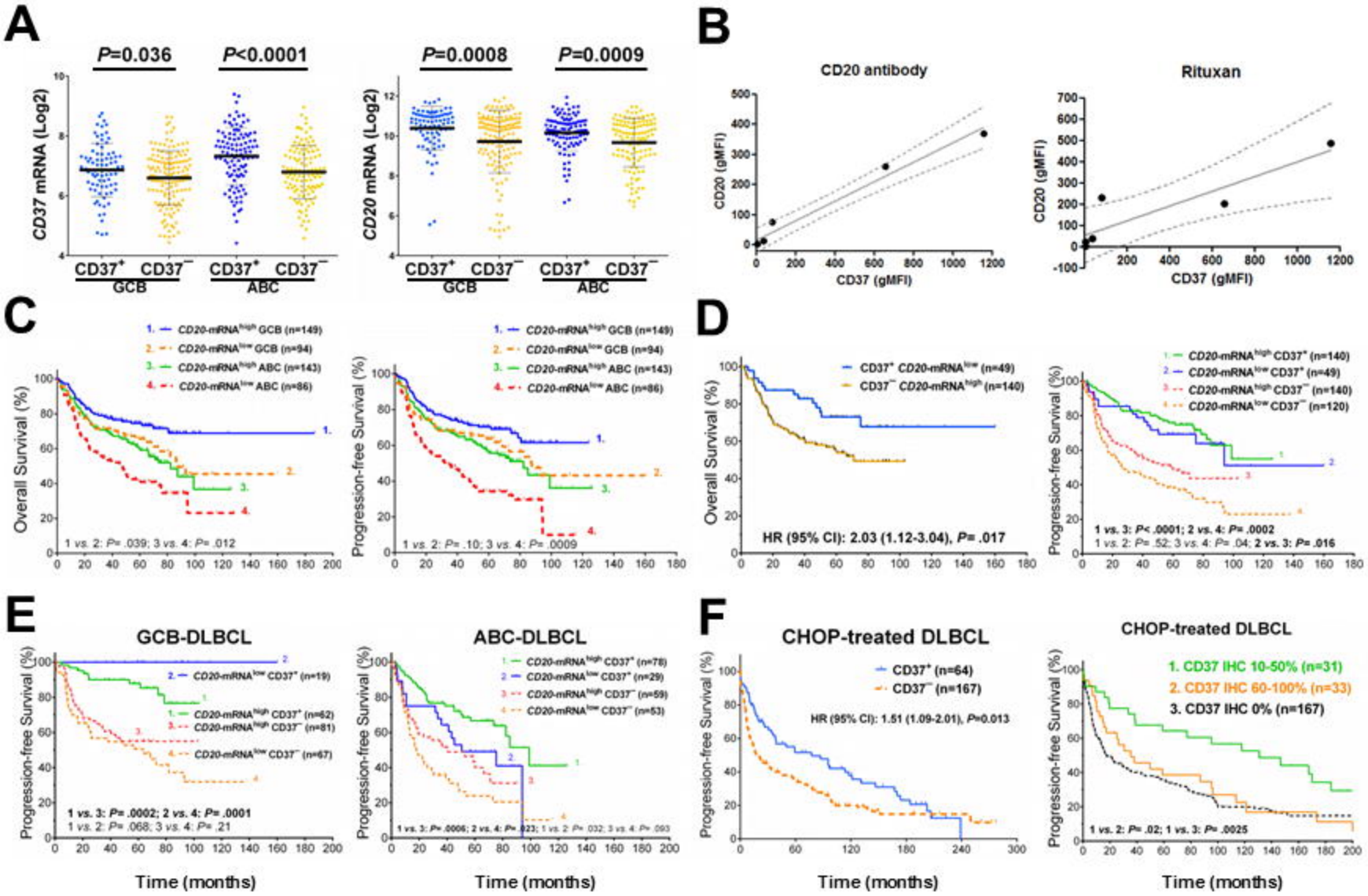
A
P=0.036
P<0.0001
P=0.0008
P=0.0009
CD37 mRNA (Log2)
CD20 mRNA (Log2)
CD37+ CD37− CD37+ CD37−
GCB
ABC
B
CD20 antibody
Rituxan
CD20 (gMFI)
CD37 (gMFI)
C
1. CD20-mRNAhigh GCB (n=149)
2. CD20-mRNAlow GCB (n=94)
3. CD20-mRNAhigh ABC (n=143)
4. CD20-mRNAlow ABC (n=86)
Overall Survival (%)
Progression-free Survival (%)
1 vs. 2: P= .039; 3 vs. 4: P= .012
1 vs. 2: P= .10; 3 vs. 4: P= .0009
D
CD37+ CD20-mRNAlow (n=49)
CD37− CD20-mRNAhigh (n=140)
HR (95% CI): 2.03 (1.12-3.04), P= .017
1. CD20-mRNAhigh CD37+ (n=140)
2. CD20-mRNAlow CD37+ (n=49)
3. CD20-mRNAhigh CD37− (n=140)
4. CD20-mRNAlow CD37− (n=120)
1 vs. 3: P< .0001; 2 vs. 4: P= .0002
1 vs. 2: P= .52; 3 vs. 4: P= .04; 2 vs. 3: P= .016
E
GCB-DLBCL
ABC-DLBCL
2. CD20-mRNAlow CD37+ (n=19)
1. CD20-mRNAhigh CD37+ (n=62)
3. CD20-mRNAhigh CD37− (n=81)
4. CD20-mRNAlow CD37− (n=67)
1 vs. 3: P= .0002; 2 vs. 4: P= .0001
1 vs. 2: P= .068; 3 vs. 4: P= .21
1. CD20-mRNAhigh CD37+ (n=78)
2. CD20-mRNAlow CD37+ (n=29)
3. CD20-mRNAhigh CD37− (n=59)
4. CD20-mRNAlow CD37− (n=53)
1 vs. 3: P= .0006; 2 vs. 4: P= .023; 1 vs. 2: P= .032; 3 vs. 4: P= .093
Progression-free Survival (%)
Time (months)
F
CHOP-treated DLBCL
CD37+ (n=64)
CD37− (n=167)
HR (95% CI): 1.51 (1.09-2.01), P=0.013
1. CD37 IHC 10-50% (n=31)
2. CD37 IHC 60-100% (n=33)
3. CD37 IHC 0% (n=167)
1 vs. 2: P= .02; 1 vs. 3: P= .0025

Fig. 3

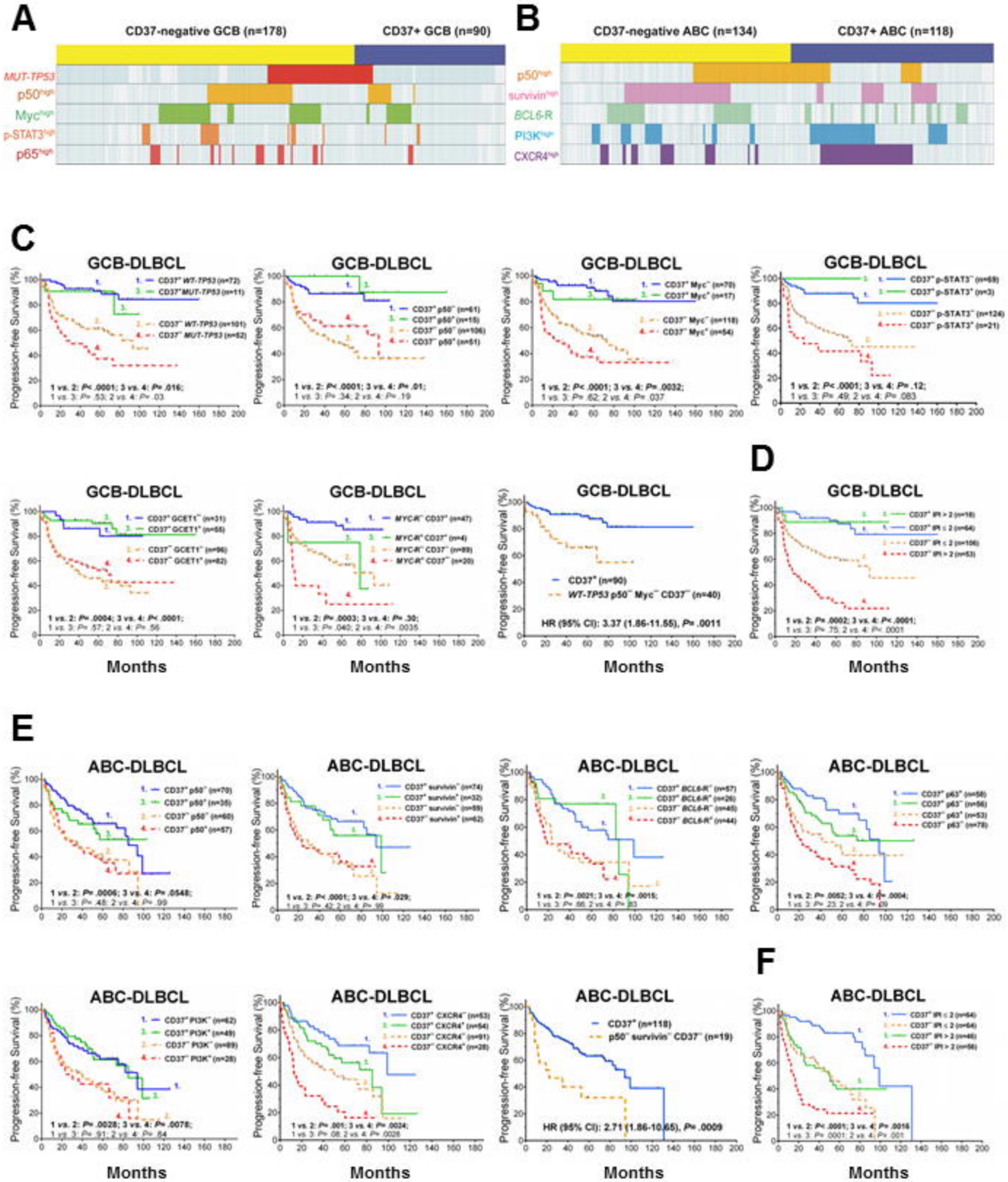
A
CD37-negative GCB (n=178)
CD37+ GCB (n=90)
MUT-TP53
p50high
Mychigh
p-STAT3high
p65high
B
CD37-negative ABC (n=134)
CD37+ ABC (n=118)
p50high
survivinhigh
BCL6-R
PI3Khigh
CXCR4high
C
GCB-DLBCL
Progression-free Survival (%)
1. CD37+ WT-TP53 (n=72)
3. CD37+ MUT-TP53 (n=11)
2. CD37− WT-TP53 (n=101)
4. CD37− MUT-TP53 (n=62)
1 vs. 2: P< .0001; 3 vs. 4: P= .016;
1 vs. 3: P= .53; 2 vs. 4: P= .03
1. CD37+ p50− (n=61)
3. CD37+ p50+ (n=15)
2. CD37− p50− (n=106)
4. CD37− p50+ (n=51)
1 vs. 2: P< .0001; 3 vs. 4: P= .01;
1 vs. 3: P= .34; 2 vs. 4: P= .19
1. CD37+ Myc− (n=70)
3. CD37+ Myc+ (n=17)
2. CD37− Myc− (n=118)
4. CD37− Myc+ (n=54)
1 vs. 2: P< .0001; 3 vs. 4: P= .0032;
1 vs. 3: P= .62; 2 vs. 4: P= .037
1. CD37+ p-STAT3− (n=69)
3. CD37+ p-STAT3+ (n=3)
2. CD37− p-STAT3− (n=124)
4. CD37− p-STAT3+ (n=21)
1 vs. 2: P< .0001; 3 vs. 4: P= .12;
1 vs. 3: P= .49; 2 vs. 4: P= .083
GCB-DLBCL
1. CD37+ GCET1− (n=31)
3. CD37+ GCET1+ (n=56)
2. CD37− GCET1+ (n=96)
4. CD37− GCET1+ (n=62)
1 vs. 2: P= .0004; 3 vs. 4: P< .0001;
1 vs. 3: P= .57; 2 vs. 4: P= .56
1. MYC/R− CD37+ (n=47)
3. MYC/R+ CD37+ (n=4)
2. MYC/R− CD37− (n=89)
4. MYC/R+ CD37− (n=20)
1 vs. 2: P= .0003; 3 vs. 4: P= .30;
1 vs. 3: P= .040; 2 vs. 4: P= .0035
CD37+ (n=90)
WT-TP53 p50− Myc− CD37− (n=40)
HR (95% CI): 3.37 (1.86-11.55), P= .0011
Months
D
GCB-DLBCL
Progression-free Survival (%)
3. CD37+ IPI > 2 (n=18)
1. CD37+ IPI ≤ 2 (n=64)
2. CD37− IPI ≤ 2 (n=106)
4. CD37− IPI > 2 (n=53)
1 vs. 2: P= .0002; 3 vs. 4: P< .0001;
1 vs. 3: P= .75; 2 vs. 4: P< .0001
Months
E
ABC-DLBCL
Progression-free Survival (%)
1. CD37+ p50− (n=70)
3. CD37+ p50+ (n=35)
2. CD37− p50− (n=60)
4. CD37− p50+ (n=57)
1 vs. 2: P= .0006; 3 vs. 4: P= .0548;
1 vs. 3: P= .48; 2 vs. 4: P= .99
1. CD37+ survivin− (n=74)
3. CD37+ survivin+ (n=32)
2. CD37− survivin− (n=89)
4. CD37− survivin+ (n=62)
1 vs. 2: P< .0001; 3 vs. 4: P= .029;
1 vs. 3: P= .42; 2 vs. 4: P= .99
1. CD37+ BCL6-R− (n=67)
3. CD37+ BCL6-R+ (n=26)
2. CD37− BCL6-R− (n=45)
4. CD37− BCL6-R+ (n=44)
1 vs. 2: P= .0021; 3 vs. 4: P= .0015;
1 vs. 3: P= .66; 2 vs. 4: P= .83
1. CD37+ p63− (n=58)
3. CD37+ p63+ (n=66)
2. CD37− p63+ (n=53)
4. CD37− p63+ (n=78)
1 vs. 2: P= .0052; 3 vs. 4: P= .0004;
1 vs. 3: P= .23; 2 vs. 4: P= .09
ABC-DLBCL
1. CD37+ PI3K− (n=62)
3. CD37+ PI3K+ (n=49)
2. CD37− PI3K− (n=89)
4. CD37− PI3K+ (n=28)
1 vs. 2: P= .0028; 3 vs. 4: P= .0078;
1 vs. 3: P= .91; 2 vs. 4: P= .84
1. CD37+ CXCR4− (n=53)
3. CD37+ CXCR4+ (n=64)
2. CD37− CXCR4− (n=91)
4. CD37− CXCR4+ (n=28)
1 vs. 2: P= .001; 3 vs. 4: P= .0024;
1 vs. 3: P= .08; 2 vs. 4: P= .0028
CD37+ (n=118)
p50− survivin− CD37− (n=19)
HR (95% CI): 2.71 (1.86-10.65), P= .0009
Months
F
ABC-DLBCL
Progression-free Survival (%)
1. CD37+ IPI ≤ 2 (n=64)
2. CD37− IPI ≤ 2 (n=64)
3. CD37+ IPI > 2 (n=46)
4. CD37− IPI > 2 (n=56)
1 vs. 2: P< .0001; 3 vs. 4: P= .0016
1 vs. 3: P= .0001; 2 vs. 4: P= .001
Months

Fig. 4

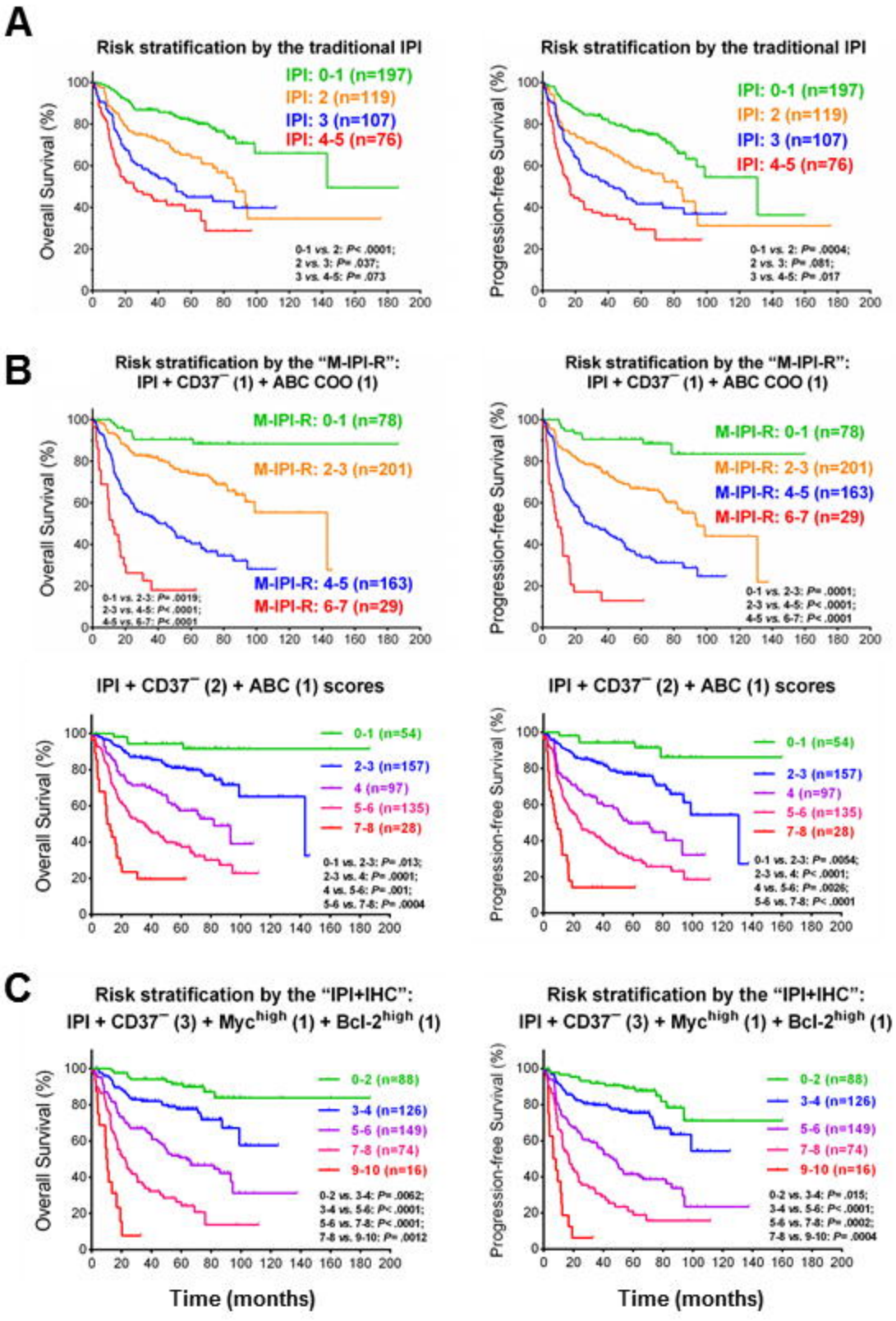
A
Risk stratification by the traditional IPI
Overall Survival (%)
IPI: 0-1 (n=197)
IPI: 2 (n=119)
IPI: 3 (n=107)
IPI: 4-5 (n=76)
0-1 vs. 2: P< .0001;
2 vs. 3: P= .037;
3 vs. 4-5: P= .073
Risk stratification by the traditional IPI
Progression-free Survival (%)
IPI: 0-1 (n=197)
IPI: 2 (n=119)
IPI: 3 (n=107)
IPI: 4-5 (n=76)
0-1 vs. 2: P= .0004;
2 vs. 3: P= .081;
3 vs. 4-5: P= .017
B
Risk stratification by the "M-IPI-R":
IPI + CD37⁻ (1) + ABC COO (1)
Overall Survival (%)
M-IPI-R: 0-1 (n=78)
M-IPI-R: 2-3 (n=201)
M-IPI-R: 4-5 (n=163)
M-IPI-R: 6-7 (n=29)
0-1 vs. 2-3: P= .0019;
2-3 vs. 4-5: P< .0001;
4-5 vs. 6-7: P< .0001
Risk stratification by the "M-IPI-R":
IPI + CD37⁻ (1) + ABC COO (1)
Progression-free Survival (%)
M-IPI-R: 0-1 (n=78)
M-IPI-R: 2-3 (n=201)
M-IPI-R: 4-5 (n=163)
M-IPI-R: 6-7 (n=29)
0-1 vs. 2-3: P= .0001;
2-3 vs. 4-5: P< .0001;
4-5 vs. 6-7: P< .0001
IPI + CD37⁻ (2) + ABC (1) scores
Overall Surival (%)
0-1 (n=54)
2-3 (n=157)
4 (n=97)
5-6 (n=135)
7-8 (n=28)
0-1 vs. 2-3: P= .013;
2-3 vs. 4: P= .0001;
4 vs. 5-6: P= .001;
5-6 vs. 7-8: P= .0004
IPI + CD37⁻ (2) + ABC (1) scores
Progression-free Survival (%)
0-1 (n=54)
2-3 (n=157)
4 (n=97)
5-6 (n=135)
7-8 (n=28)
0-1 vs. 2-3: P= .0054;
2-3 vs. 4: P< .0001;
4 vs. 5-6: P= .0026;
5-6 vs. 7-8: P< .0001
C
Risk stratification by the "IPI+IHC":
IPI + CD37⁻ (3) + Myc^high (1) + Bcl-2^high (1)
Overall Survival (%)
0-2 (n=88)
3-4 (n=126)
5-6 (n=149)
7-8 (n=74)
9-10 (n=16)
0-2 vs. 3-4: P= .0062;
3-4 vs. 5-6: P< .0001;
5-6 vs. 7-8: P< .0001;
7-8 vs. 9-10: P= .0012
Risk stratification by the "IPI+IHC":
IPI + CD37⁻ (3) + Myc^high (1) + Bcl-2^high (1)
Progression-free Survival (%)
0-2 (n=88)
3-4 (n=126)
5-6 (n=149)
7-8 (n=74)
9-10 (n=16)
0-2 vs. 3-4: P= .015;
3-4 vs. 5-6: P< .0001;
5-6 vs. 7-8: P= .0002;
7-8 vs. 9-10: P= .0004
Time (months)
Time (months)

Fig. 5

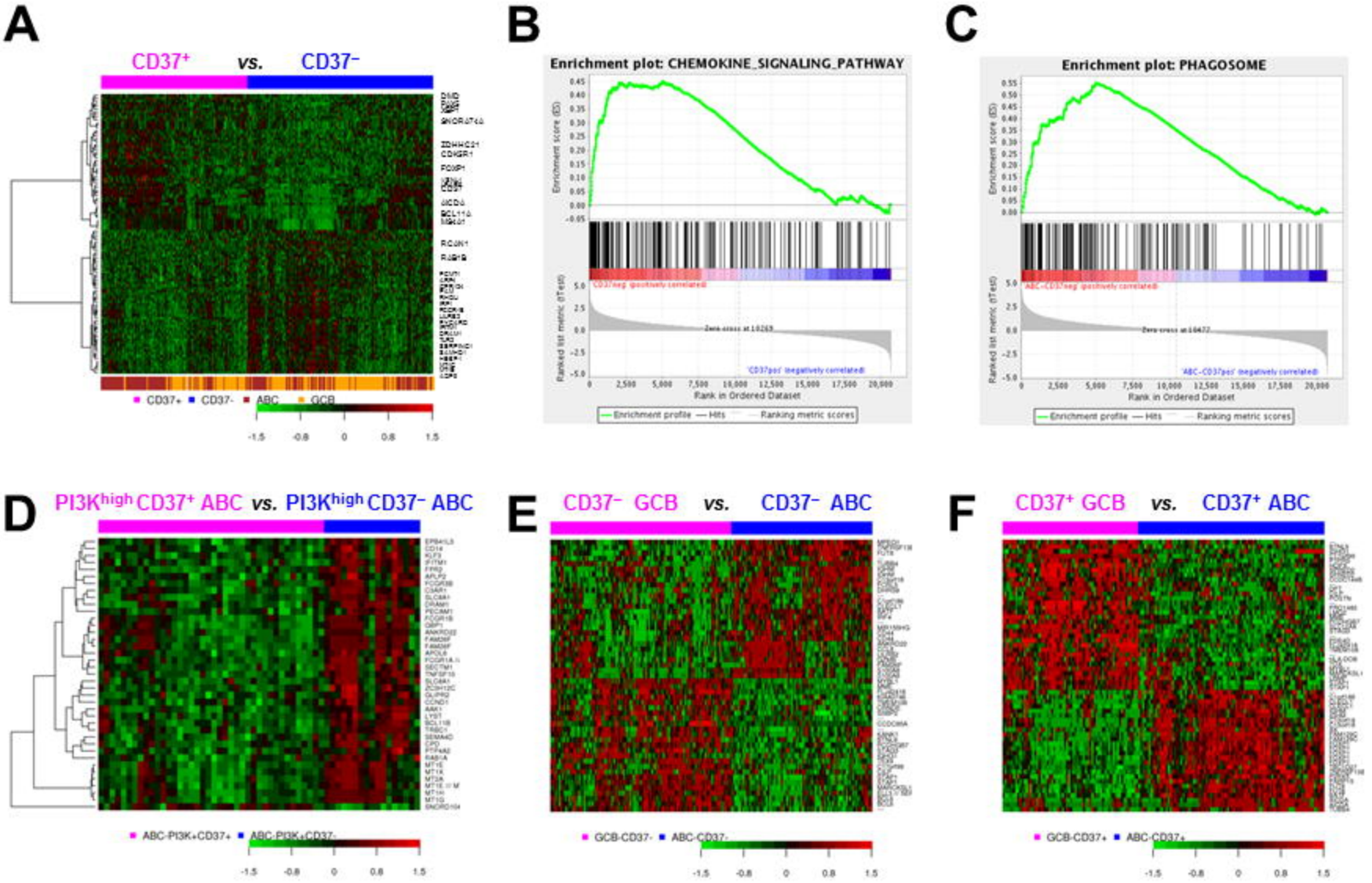
A
CD37+ vs. CD37−
CD37+ CD37- ABC GCB
-1.5 -0.8 0 0.8 1.5
B
Enrichment plot: CHEMOKINE_SIGNALING_PATHWAY
Enrichment score (ES)
Ranked list metric (tTest)
Rank in Ordered Dataset
Enrichment profile Hits Ranking metric scores
C
Enrichment plot: PHAGOSOME
Enrichment score (ES)
Ranked list metric (tTest)
Rank in Ordered Dataset
Enrichment profile Hits Ranking metric scores
D
PI3Khigh CD37+ ABC vs. PI3Khigh CD37− ABC
ABC-PI3K+CD37+ ABC-PI3K+CD37-
-1.5 -0.8 0 0.8 1.5
E
CD37− GCB vs. CD37− ABC
GCB-CD37- ABC-CD37-
-1.5 -0.8 0 0.8 1.5
F
CD37+ GCB vs. CD37+ ABC
GCB-CD37+ ABC-CD37+
-1.5 -0.8 0 0.8 1.5

Fig. 6

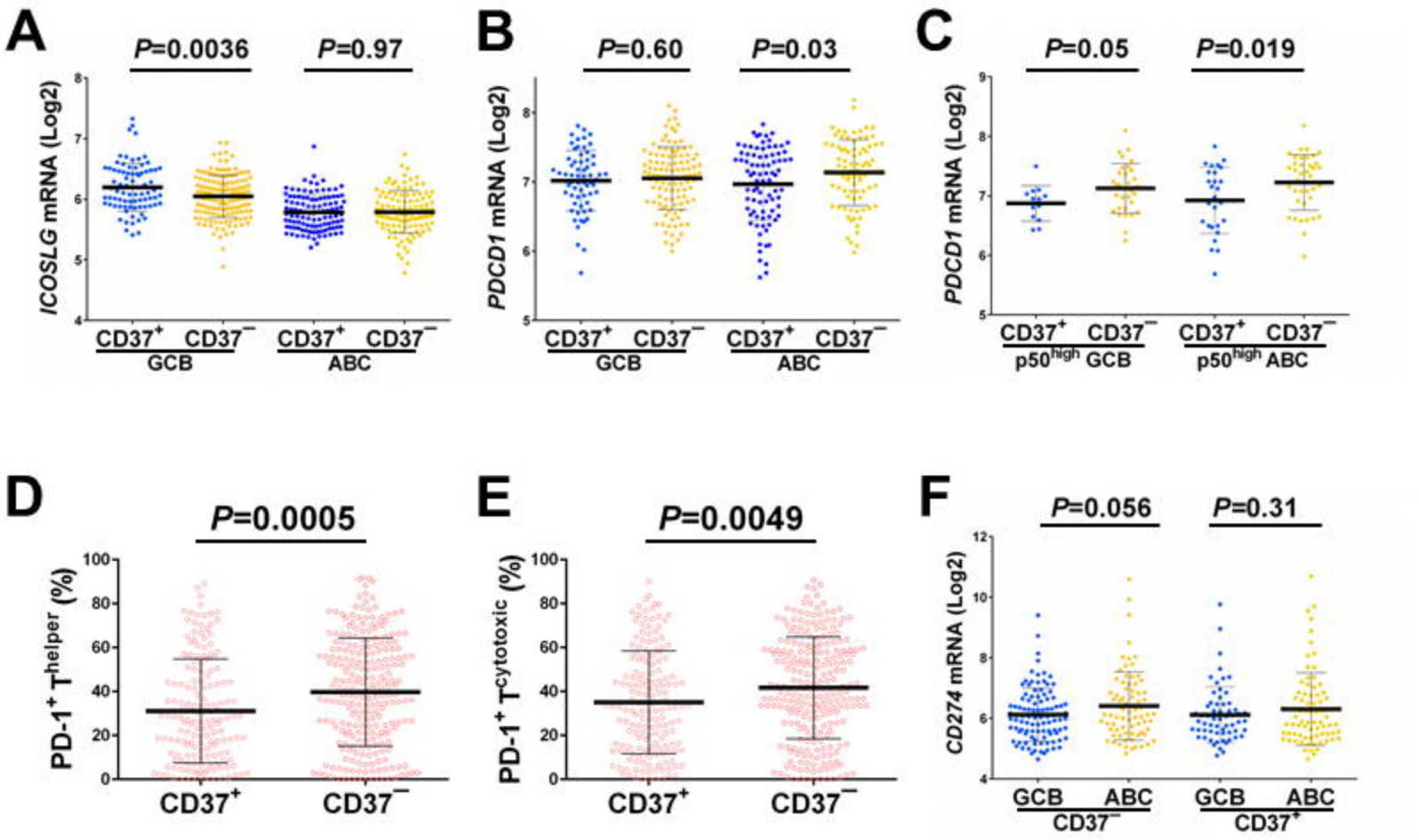
A
P=0.0036
P=0.97
ICOSLG mRNA (Log2)
CD37+ CD37−
GCB
CD37+ CD37−
ABC
B
P=0.60
P=0.03
PDCD1 mRNA (Log2)
CD37+ CD37−
GCB
CD37+ CD37−
ABC
C
P=0.05
P=0.019
PDCD1 mRNA (Log2)
CD37+ CD37−
p50high GCB
CD37+ CD37−
p50high ABC
D
P=0.0005
PD-1+ Thelper (%)
CD37+
CD37−
E
P=0.0049
PD-1+ Tcytotoxic (%)
CD37+
CD37−
F
P=0.056
P=0.31
CD274 mRNA (Log2)
GCB ABC
CD37−
GCB ABC
CD37+

Fig. 7

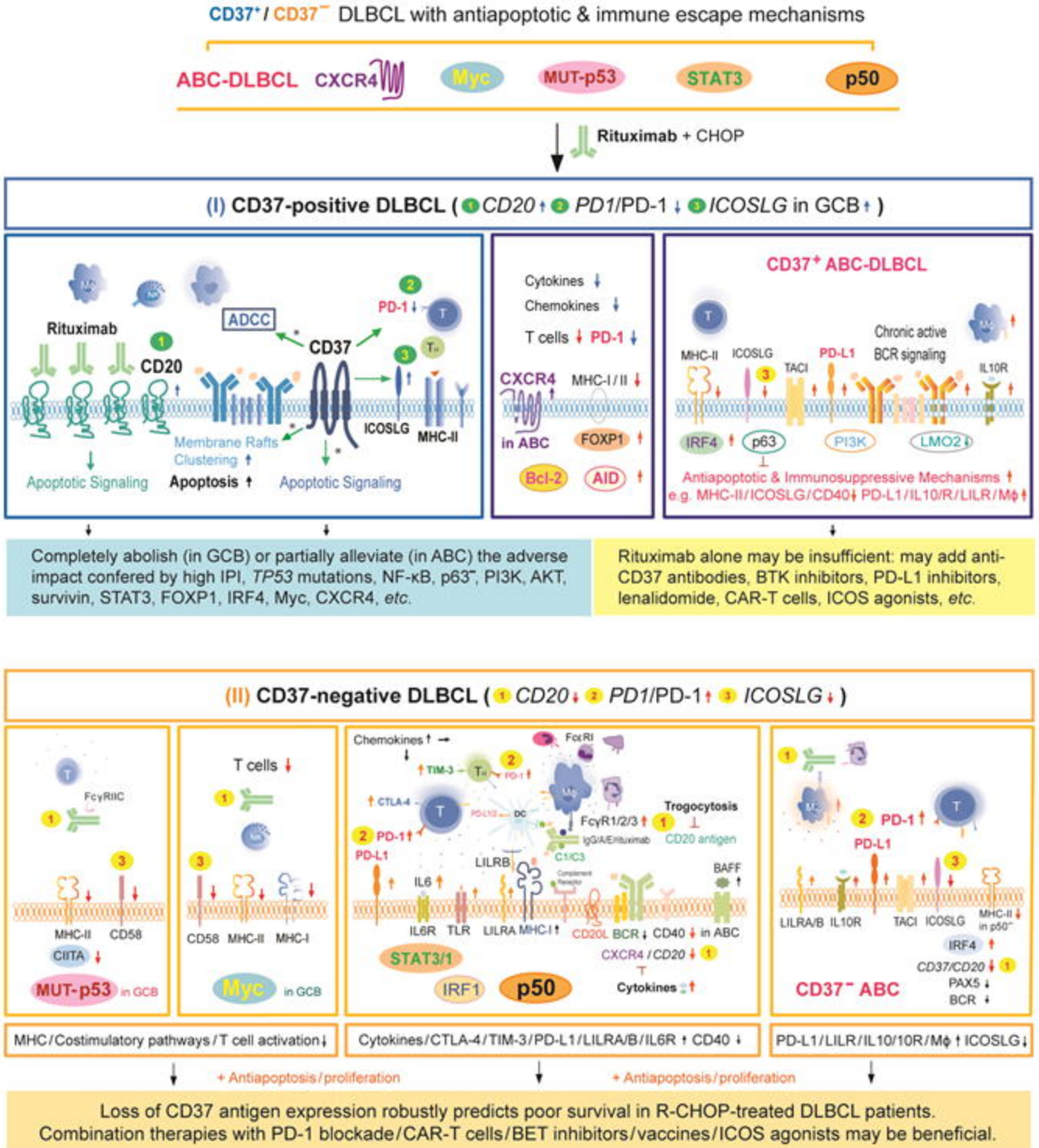
CD37+ / CD37− DLBCL with antiapoptotic & immune escape mechanisms
ABC-DLBCL
CXCR4
Myc
MUT-p53
STAT3
p50
Rituximab + CHOP
(I) CD37-positive DLBCL (1 CD20↑ 2 PD1/PD-1↓ 3 ICOSLG in GCB↑)
Rituximab
CD20
ADCC
CD37
PD-1↓
ICOSLG
MHC-II
Membrane Rafts Clustering ↑
Apoptotic Signaling
Apoptosis ↑
Apoptotic Signaling
Cytokines ↓
Chemokines ↓
T cells ↓ PD-1 ↓
CXCR4 in ABC
MHC-I / II ↓
FOXP1 ↑
Bcl-2
AID ↑
CD37+ ABC-DLBCL
MHC-II
ICOSLG
TACI
PD-L1
Chronic active BCR signaling
IL10R
IRF4 ↑
p63
PI3K
LMO2↓
Antiapoptotic & Immunosuppressive Mechanisms ↑
e.g. MHC-II/ICOSLG/CD40↓ PD-L1/IL10/R/LILR/Mϕ↑
Completely abolish (in GCB) or partially alleviate (in ABC) the adverse impact confered by high IPI, TP53 mutations, NF-κB, p63−, PI3K, AKT, survivin, STAT3, FOXP1, IRF4, Myc, CXCR4, etc.
Rituximab alone may be insufficient: may add anti-CD37 antibodies, BTK inhibitors, PD-L1 inhibitors, lenalidomide, CAR-T cells, ICOS agonists, etc.
(II) CD37-negative DLBCL (1 CD20↓ 2 PD1/PD-1↑ 3 ICOSLG↓)
FcγRIIC
MHC-II
CD58
CIITA ↓
MUT-p53 in GCB
T cells ↓
CD58
MHC-II
MHC-I
Myc in GCB
Chemokines ↑
FcεRI
TIM-3 ↑
PD-1 ↑
CTLA-4 ↑
PD-L1/2
DC
FcγR1/2/3 ↑
Trogocytosis
IgG/A/E/rituximab
CD20 antigen
PD-1↑
PD-L1
LILRB
C1/C3
IL6 ↑
BAFF ↑
IL6R
TLR
LILRA
MHC-I ↑
CD20L
BCR ↓
CD40 ↓ in ABC
CXCR4 / CD20 ↓
STAT3/1
IRF1
p50
Cytokines ↕↑
PD-1↑
PD-L1
LILRA/B
IL10R
TACI
ICOSLG
MHC-II in p50−
IRF4 ↑
CD37/CD20 ↓
PAX5 ↓
BCR ↓
CD37− ABC
MHC/Costimulatory pathways/T cell activation↓
Cytokines/CTLA-4/TIM-3/PD-L1/LILRA/B/IL6R ↑ CD40 ↓
PD-L1/LILR/IL10/10R/Mϕ ↑ ICOSLG↓
+ Antiapoptosis/proliferation
+ Antiapoptosis/proliferation
Loss of CD37 antigen expression robustly predicts poor survival in R-CHOP-treated DLBCL patients.
Combination therapies with PD-1 blockade/CAR-T cells/BET inhibitors/vaccines/ICOS agonists may be beneficial.